BIOPROBES 52

MARCH 2007

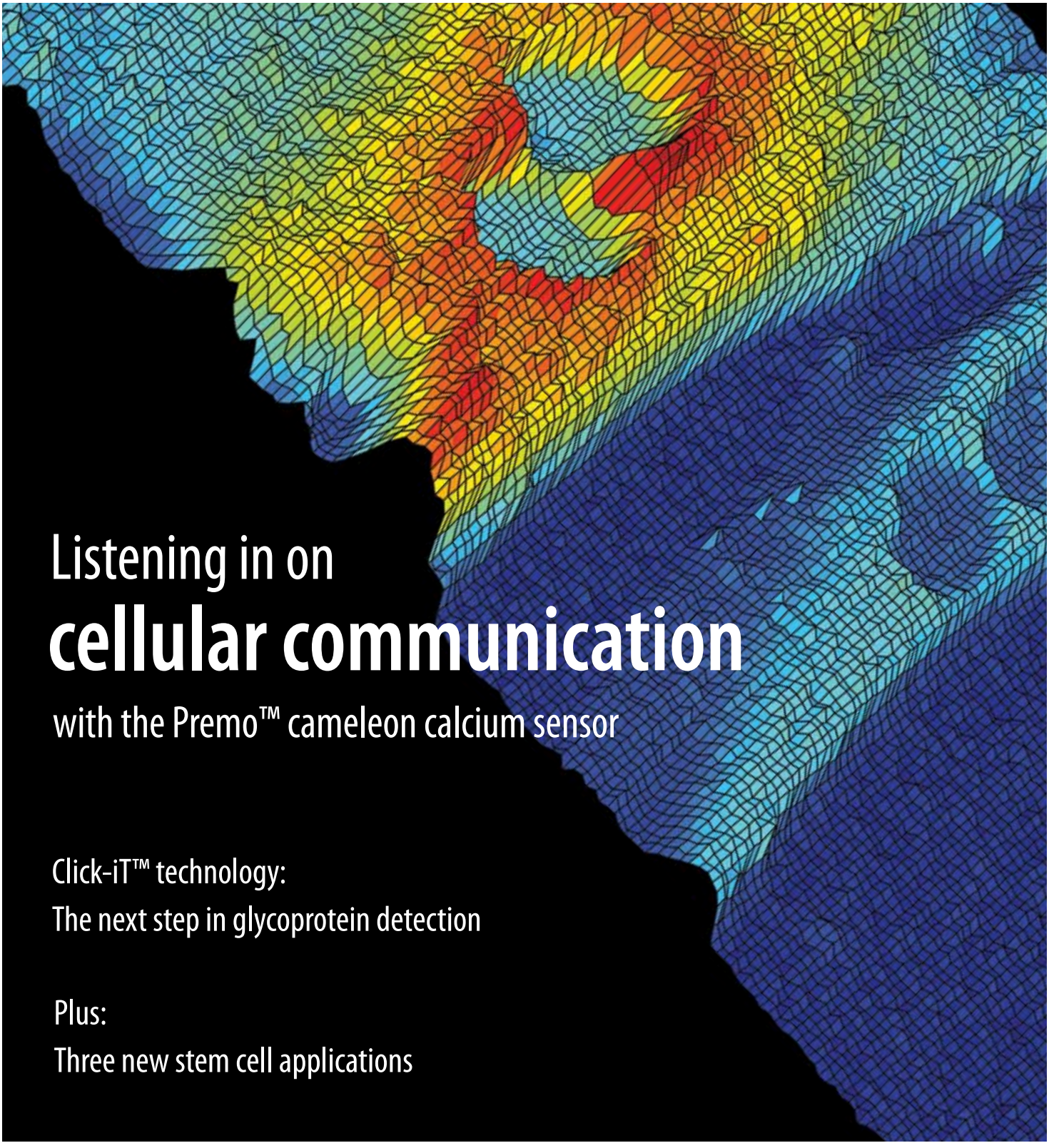

Listening in on cellular communication

with the Premo™ cameleon calcium sensor

Click-iT™ technology:
The next step in glycoprotein detection

Plus:
Three new stem cell applications

invitrogen™

Molecular Probes®
invitrogen detection technologies

Molecular Probes
29851 Willow Creek Road
Eugene, OR 97402

PREVIOUS ISSUES

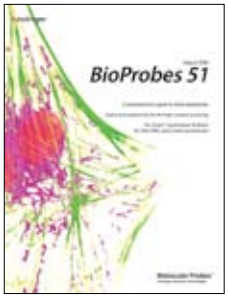

BioProbes 51

This issue describes more than 250 products for applications in immunodetection, flow cytometry, and imaging analysis. Read about a complete, integrated solution for DNA, RNA, and protein quantitation; sift through the options for primary and secondary antibody detection; and get a rundown of 100 probes for membrane research.

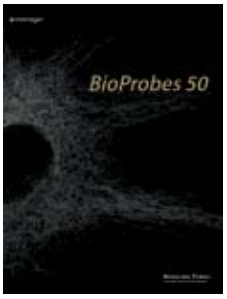

BioProbes 50

The 50th issue of *BioProbes* features an in-depth look at nanocrystal technology, a summary of Invitrogen™ flow cytometry products, a comprehensive guide to our diverse selection of probes for neuroscience applications, and descriptions of 75 new products.

BioProbes 49

Whether your area of interest is flow cytometry, imaging analysis, molecular biology, or biochemistry, you'll find descriptions of products and applications in *BioProbes 49* that can take your work in a new direction.

Back issues of *BioProbes* published after 1995 are available at **probes.invitrogen.com/bioprobes**.

ProbesOnline

Get the latest news about Molecular Probes® products and applications every month in *ProbesOnline*, the opt-in e-newsletter from Invitrogen. To subscribe, send a blank email to **ProbesOnline-subscribe@invitrogen.com**.

Published by Molecular Probes, Inc.
Eugene, Oregon USA © 2007

BioProbes® newsletter is published several times each year by Molecular Probes, Inc. *BioProbes* is dedicated to furnishing researchers with the very latest information about Molecular Probes® products and their applications. For a listing of our products, along with extensive descriptions and literature references, please see our website. Prices are subject to change without notice. Quantity discounts may be available.

Editor
Jennifer Bordun

Contributing Editors
Jay Gregory, Ph.D.
Robyn Leung, M.S.
Coleen Miller, Ph.D.
Grace Richter, Ph.D.
Michelle T.Z. Spence, Ph.D.

Contributing Writers
Beth Browne, Ph.D.
Stephen Chamberlain, Ph.D.
W. Gregory Cox, Ph.D.
Jeffrey Croissant, Ph.D.
Kathleen Free
Maura Ford, M.S.
Kenton Gregory, Ph.D.
George Hanson, Ph.D.
Sara Hereley
Michael Janes, M.S.
Iain Johnson, Ph.D.
Louis Leong, Ph.D.
Julie Nyhus, M.S.
Michael O'Grady, Ph.D.
David Phan, Ph.D.
Xiao-Dong Qian, Ph.D
Steve Riddle
Michael Rutten, Ph.D.
Erik Schaefer, Ph.D.
Soojung Shin, Ph.D., D.V.M.
Tom Steinberg, Ph.D.
Mark Surby, Ph.D.
Chip Walker, Ph.D.
Patricia Whaley, Ph.D.

Design
Lynn Soderberg

Cover Design
Kelly Christensen

Figures and Images
Christopher Barnhart
Shayne Boucher, Ph.D.
Jolene Bradford
Ian Clements, M.S.
Maura Ford, M.S.
William Godfrey, Ph.D.
Kenton Gregory, M.D.
George Hanson, Ph.D.
Courtenay Hart
Louis Leong, Ph.D.
Julie Nyhus, M.S.
Michael O'Grady, Ph.D.
Xiao-Dong Qian, Ph.D
Matthew Robers, M.S.
Michael Rutten, Ph.D.
Soojung Shin, Ph.D., D.V.M.
Bethany Sutton, M.S.
Mark Surby, Ph.D.
Will Westra
Pamela Whitney

Molecular Probes®
invitrogen detection technologies

probes.invitrogen.com

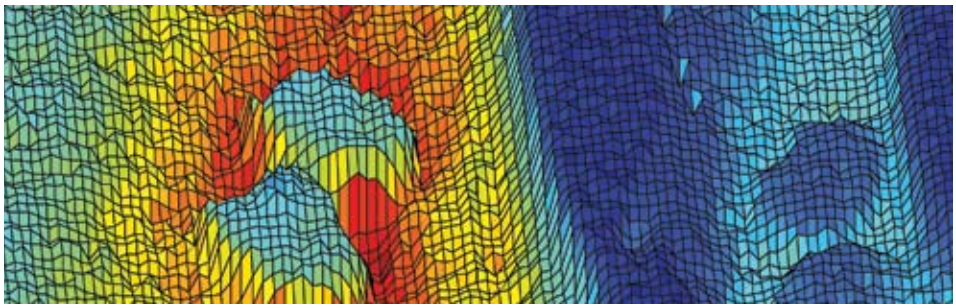

BioProbes 52

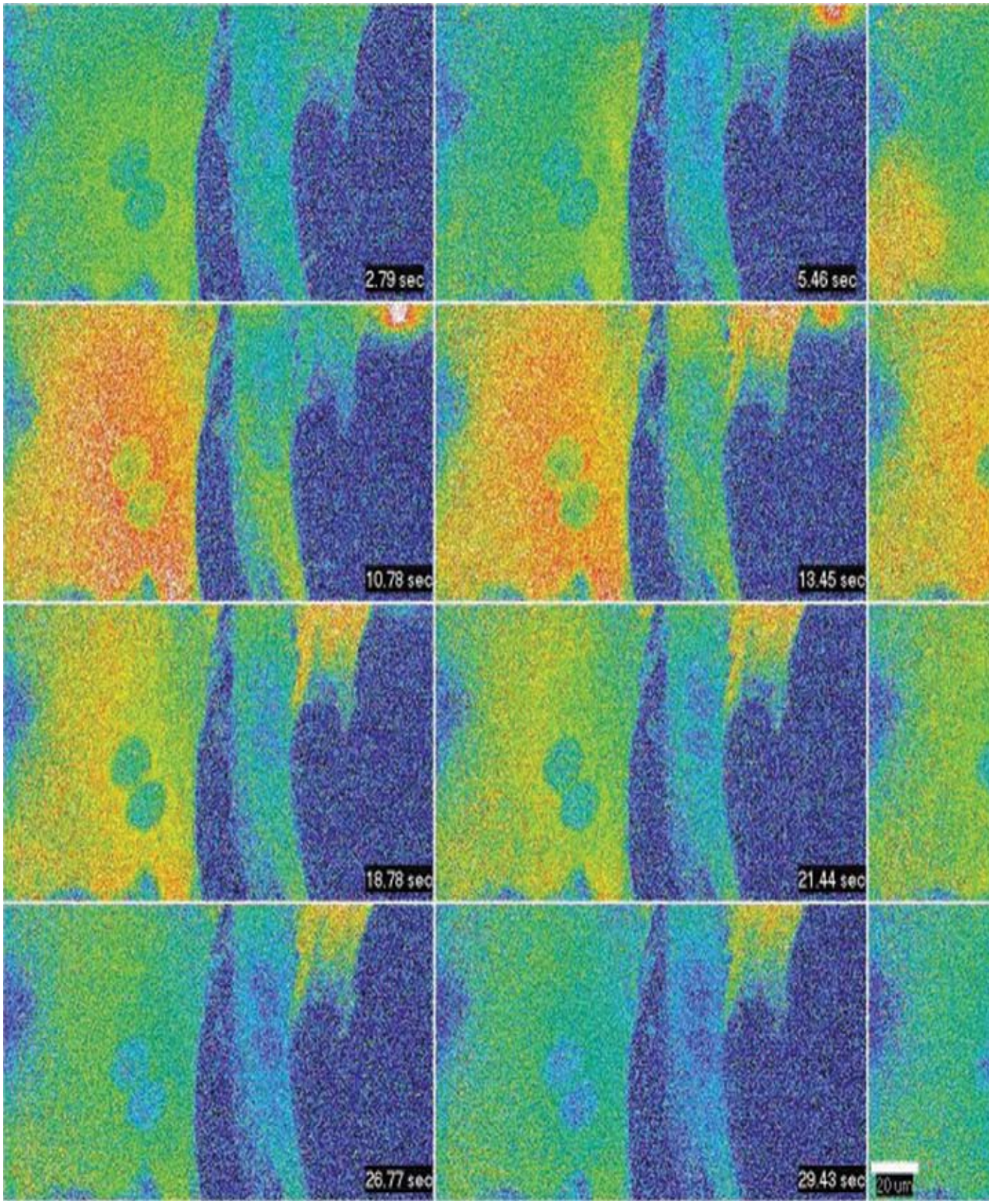

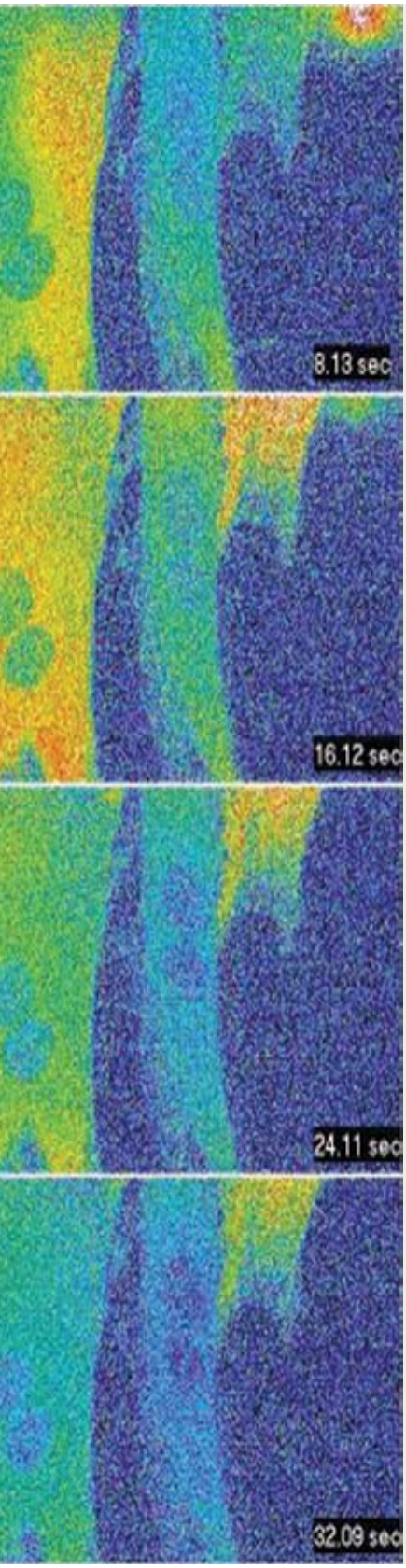

Listening in on cellular communication

PREMO™ CAMELEON CALCIUM SENSOR.

Cells are constantly talking. Extracellular signals such as hormones and neurotransmitters convey a barrage of information to the cell that is crucial for its survival and function. Within the cell, second messengers like Ca^{2+} and cAMP relay these extracellular signals to proteins that translate the signals into action. To be able to measure such dynamic signaling events within a cell in real time is to eavesdrop on the functional language of the cell in its native state. A variety of ion indicator molecules exist to allow certain insights into these important pathways and processes; however, there has not been a widely available genetically encoded tool to expand researchers' capabilities into targeted and iterative measurements. With the release of the Premo™ cameleon calcium sensor, a genetically encoded, fluorescence resonance energy transfer (FRET)–based tool for ratiometric measurement of Ca^{2+} is now available. →

Figure 1—Live-cell calcium imaging using the Premo™ cameleon calcium sensor. Porcine left atrial appendage (LAA) progenitor cells were transduced with the Premo™ cameleon calcium sensor, incubated overnight at 37°C, and imaged at 3 second intervals before and after stimulation with 10 µM ATP using a Zeiss® LSM 5 LIVE microscope. The time-lapse sequence of intensity profile images illustrates changes in YFP and CFP signal levels, which are pseudocolored to indicate Ca^{2+} flux. Images obtained in collaboration with Michael Rutten and Kenton Gregory, Oregon Medical Laser Center Bioimaging Suite, Providence St. Vincent Hospital, Portland, Oregon.

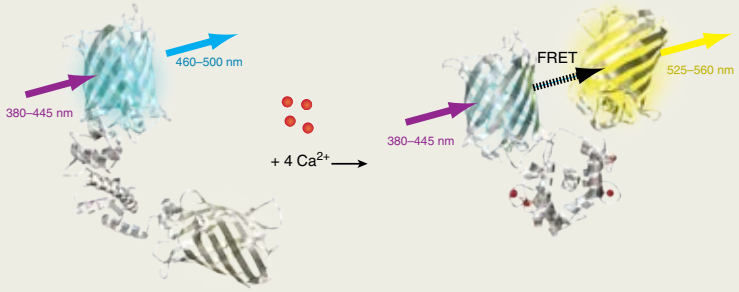

Figure 2—Schematic of the Premo™ cameleon calcium sensor mechanism.

The BacMam delivery system uses baculovirus to deliver the sensor into cells of interest and has been shown to be an efficient transducer of a wide range of mammalian cell types [4] (see **www.invitrogen.com/premo** for a full list), including stem cells and primary cells that have proven difficult to transfect or transduce by other methods. The delivery system is currently not effective in hematopoietic or macrophage cells. The Premo™ cameleon calcium sensor is provided as a ready-to-use solution of virus that is used in conjunction with the included Premo™ enhancer for increased expression of the cameleon sensor. The sensor provides an effective technique for measuring Ca^{2+} mobilization in transduced cells using microplate-based assays or fluorescence microscopy. Figure 5 illustrates the utility of the probe in agonist and antagonist modes for the measurement of Ca^{2+} in a microplate-based assay.

Interpret cell signaling in real time

The Premo™ cameleon calcium sensor combines a genetically encoded FRET-based calcium sensor with efficient BacMam (baculovirus) delivery to measure intracellular calcium in live-cell studies [1] (Figure 1). The sensor is based on the YC3.60 version of the cameleon family developed by Tsien, Miyawaki, and coworkers [2,3] (Figure 2). Binding of four Ca^{2+} ions to the calmodulin portion of the sensor induces a conformational change that brings Cyan Fluorescent Protein (CFP) and Yellow Fluorescent Protein (YFP-cpVenus) closer to each other, allowing FRET to occur. This leads to an increase in YFP emission (535 nm) and a decrease in CFP emission (485 nm) indicative of Ca^{2+} release in the system under study (Figure 3). The ratiometric aspect of the readout (Figure 4) helps eliminate assay variations due to autofluorescence or differences in fluorescence between samples.

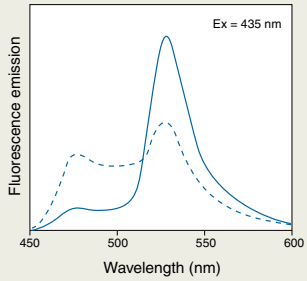

Figure 3—Fluorescence emission spectra of Premo™ cameleon calcium sensor. The dashed line indicates the spectra in the absence of Ca^{2+}; the solid line shows the fluorescence resonance energy transfer (FRET)-based change upon Ca^{2+} binding.

Real cells, real insight

Important advances in understanding cell signaling have led to new targeted therapies for cancer and other disease states, and continue to point toward interesting possibilities for new probes to map these pathways.[5,6] Tools for measuring Ca^{2+} are widely available and used routinely in research laboratories and for drug screening; however, these have been primarily limited to applications based on binding of the ion to a small chemical entity (e.g., fluo-3 and fluo-4) or to protein-based luminescent Ca^{2+} sensors (e.g., aequorin). Working with colleagues at the Oregon Medical Laser Center/Providence St. Vincent Hospital (Portland, Oregon), we have shown the capabilities of the Premo™ cameleon calcium sensor with BacMam delivery for visualizing and quantitating ATP-mediated Ca^{2+} flux in primary and progenitor cell types.

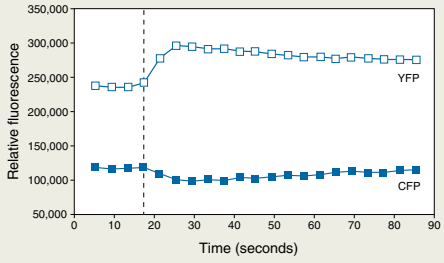

Figure 4—Example of single-well readings from a fluorescence-based microplate reader. HeLa cells were transduced with the Premo™ cameleon calcium sensor and plated in Opti-MEM® 1 medium + 1% FBS. The following day, a dose response assay for Ca^{2+} flux was performed using histamine. The agonist was injected at 16 seconds (dashed line) with readings acquired every 4–5 seconds.

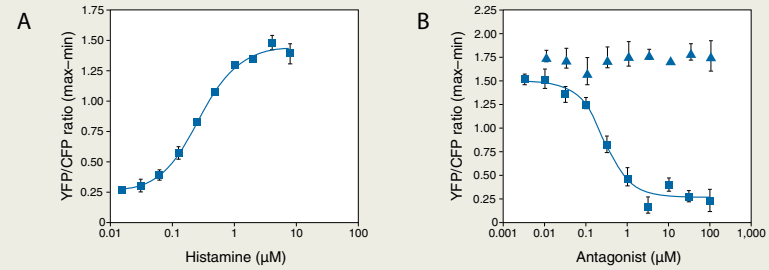

Figure 5—Agonist and antagonist dose response curves. HeLa cells were plated in a 96-well plate at a density of 15,000 cells/well, transduced with Premo™ cameleon calcium sensor, and incubated overnight at 37°C. The following day, a histamine dose response was performed (A). A separate plate was used to evaluate an antagonist dose response with pyrilamine (■) and thioperamide (▲) in the presence of an EC_{80} concentration of histamine (B). Pyrilamine is a known H1 receptor antagonist that couples through G_q proteins and the second messenger Ca^{2+}. Thioperamide is a known H3 receptor antagonist that couples through G_i proteins and the second messenger cAMP.

In this study, porcine primary cardiac and skeletal muscle cells and left atrial appendage (LAA) progenitor cells were transduced with the Premo™ cameleon calcium sensor. The cells were incubated overnight, followed by agonist induction for Ca^{2+} flux measurements. The LAA progenitor cells exhibited cytoplasmic expression as expected, and following administration of 20 µM ATP, we observed a receptor-mediated Ca^{2+} flux indicated by a change in color (Figure 1, page 2); quantitative measurements were also obtained (Figure 6). These results indicate a Ca^{2+}-dependent FRET response from the cameleon sensor. Other agonists (e.g., carbachol) and cell types were also analyzed successfully with the Premo™ cameleon calcium sensor (data not shown).

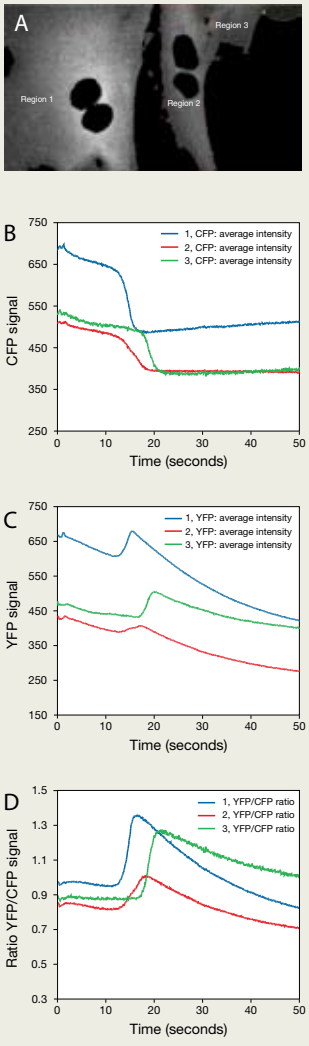

Figure 6—Analysis of YFP/CFP ratio to determine change in Ca^{2+} flux. Cells from Figure 1 were processed through a binary mask to remove the background noise and nuclear regions. The merged cell areas were divided manually, and a binary mask was used to define the regions (A). Panels B, C, and D show the change in CFP signal, YFP signal, and YFP/CFP ratio, respectively, as determined using Zeiss® LSM software.

Learn the language

The Premo™ cameleon calcium sensor pairs a fluorescent protein–based ion sensor with the very efficient, ready-to-use BacMam viral transduction delivery system to provide highly selective intracellular Ca^{2+} measurement. Building on this powerful new tool, Invitrogen plans a suite of second messenger indicators to support researchers in their quest to map and mine the dynamic events of cellular physiology. To learn more about the Premo™ cameleon calcium sensor, visit **www.invitrogen.com/premo**. ■

Michael Rutten, Ph.D., and Kenton Gregory, M.D., Oregon Medical Laser Center Bioimaging Suite, Providence St. Vincent Hospital (Portland, Oregon), contributed to this article.

References

1. Kost, T. et al. (2005) *Nat Biotechnol* 23:567–575.
2. Nagai, T. et al. (2004) *Proc Natl Acad Sci U S A* 101:10554–10559.
3. Miyawaki, A. et al. (1997) *Nature* 388:882–887.
4. Kost, T. and Condreay, J.P. (2002) *Trends Biotechnol* 20:173–180.
5. Cohen, P. (2002) *Nat Rev Drug Discov* 1:309–315.
6. Austin, C. et al. (2004) *Science* 306:1138–1139.

Product	Quantity	Cat. no.
Premo™ cameleon calcium sensor *for 10 microplates*	1 kit	P36207
Premo™ cameleon calcium sensor *for 100 microplates*	1 kit	P36208

Click. Discover. Publish.

CLICK-IT™ GLYCOPROTEIN PROFILING REAGENTS.

Click—The next generation in fluorescence labeling and detection

Fluorescence labeling and detection methods have enabled significant advancements in biomedical research by providing tools that supplant hazardous radioactive and insensitive colorimetric assays and reagents. Labeling a specific class of biomolecules in the context of a live cell or complex cell lysate, however, requires a selectivity that common reactive fluorescent probes cannot deliver. Fluorescence chemistry traditionally targets amines, sulfhydryls, and carboxylates—functional groups that are not unique to the biomolecule of interest. Indirect labeling methods that employ antibody or lectin conjugates offer the selectivity that reactive fluorescent probes lack, but this selectivity comes with several limitations. The large size of these protein conjugates severely restricts their access to intracellular compartments. Furthermore, because they are often the same size or larger than their targets, antibody and lectin conjugates potentially modify the solubility, localization, and interactions of the molecule under study. Genetically encoded fluorescent protein reporters such as Green Fluorescent Protein (GFP) and its variants circumvent the cell permeability issue by using intracellular transcription and translation machinery to label the protein, but here too the protein-sized fluorescent reporter may interfere with the normal functioning of the protein.

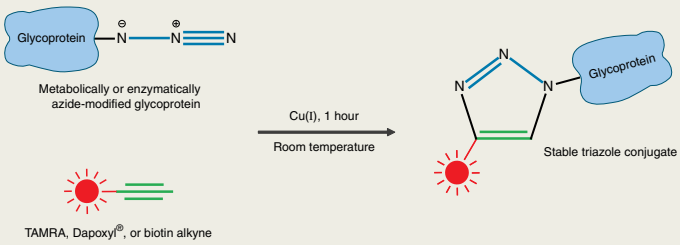

Figure 1—Click-iT™ azide/alkyne reaction.

What's needed is a chemoselective labeling technique that is compatible with complex biological systems and relatively transparent to the cell machinery. The new Click-iT™ technology employs an advanced two-step labeling method that addresses both the size of the fluorescent tag and the selectivity of the labeling reaction. Here we describe our first application of this technology: Click-iT™ glycoprotein labeling reagents and Click-iT™ Glycoprotein Detection Kits, which are based on this two-step labeling method.

In the first step, a specific class of biomolecules (in this case, glycoproteins) in an experimental sample—be it live cells, cell lysate, or protein fraction—is enzymatically labeled with an unnatural biosynthetic precursor containing a Click-iT™ azide handle. The choice of azide-containing substrate and corresponding enzyme defines the selectivity of this labeling reaction; the incorporation of the small (three-atom) azide moiety provides a bioorthogonal functional group that typically neither reacts with other cell components nor disrupts normal cell processes. If the target molecule contains a unique functional group, this first labeling step can also be accomplished nonenzymatically using a reactive azide. In the second step, molecules selectively labeled with the Click-iT™ azide handle are detected with a fluorescent or biotinylated alkyne using Cu(I)-catalyzed cycloaddition or "click" chemistry [1–4] (Figure 1). Not only is it fast, selective, and extremely efficient, but the click reaction produces a very stable covalent bond between the azide and alkyne, capable of withstanding mass spectrometry (MS) ionization.

Click-iT™ technology has far-reaching implications for a multitude of *in vivo* and *in vitro* fluorescence labeling applications. Through the selective enzymatic incorporation of a bioorthogonal Click-iT™ handle, a class of biomolecules can be tagged yet remain functional within the parameters of normal cell activity. At any point after labeling, these biomolecules can be selectively and sensitively detected using a click reaction. For example, using an azide-containing fucose analog, Sawa

and coworkers have selectively labeled fucosylated glycoconjugates via the fucose salvage pathway, detected them with an azide/alkyne click reaction using a fluorescent or biotinylated alkyne, and studied their intracellular localization by fluorescence microscopy.[5] The state-of-the-art Click-iT™ reagents allow you to completely sidestep the nonspecific binding interactions of antibodies and lectins that often plague immunolabeling experiments, as well as the potential sample destruction through β-elimination (BEMAD) and the biohazards associated with radioactivity-based detection methods.

Discover—Click-iT™ tools for glycoprotein profiling

Glycosylation is the most ubiquitous posttranslational modification of cellular proteins and yet, due to the shortcomings of existing research tools, very little is known about the role of protein glycosylation in vital cellular processes such as cell growth and differentiation, cell surface interactions, intracellular signaling, and protein stability. Harnessing the chemoselectivity of click chemistry, the new Click-iT™ glycoprotein profiling reagents provide a simple and robust two-step method for detecting and characterizing specific glycoprotein subclasses, with detection limits in the low femtomole range.

Four different Click-iT™ glycoprotein labeling reagents are available (Table 1), each providing an azide-modified sugar for biosynthetic incorporation into a specific subclass of protein glycan structures:

- Click-iT™ GalNAz metabolic glycoprotein labeling reagent, a tetraacetylated azido galactosamine for *in vivo* labeling of *O*-linked glycoproteins
- Click-iT™ ManNAz metabolic glycoprotein labeling reagent, a tetraacetylated azido mannosamine for *in vivo* labeling of cell-surface sialic acid–modified glycoproteins

Table 1—Click-iT™ glycoprotein labeling reagents.

Sample	Glycoprotein subclass	Click-iT™ labeling reagent	Cat. no.
Cultured cells	*O*-Linked	Click-iT™ GalNAz metabolic glycoprotein labeling reagent	C33365
	O-GlcNAc	Click-iT™ GlcNAz metabolic glycoprotein labeling reagent	C33367
	Sialic acid	Click-iT™ ManNAz metabolic glycoprotein labeling reagent	C33366
Pure protein, cell lysate, or protein extract	*O*-GlcNAc	Click-iT *O*-GlcNAc Enzymatic Labeling System	C33368

- Click-iT™ GlcNAz metabolic glycoprotein labeling reagent, a tetraacetylated azido glucosamine for *in vivo* labeling of intracellular *O*-linked *N*-acetylglucosamine (*O*-GlcNAc)–modified glycoproteins
- Click-iT™ *O*-GlcNAc Enzymatic Labeling System, an azido galactose for *in vitro* labeling of *O*-GlcNAc–modified glycoproteins

The Click-iT™ metabolic glycoprotein labeling reagents comprise three different tetraacetylated azido sugars, which act as biosynthetic precursors for *in vivo* labeling of three different subclasses of glycoproteins.[6–8] Cultured cells are simply incubated with the modified sugars for 2–3 days or until cells reach the appropriate density. The acetyl groups improve cell permeability of the modified sugars and are removed by nonspecific intracellular carboxylesterases. The resulting azido sugar is then metabolically incorporated into a protein glycan structure through the permissive nature of the oligosaccharide biosynthesis pathway, yielding a glycoprotein containing the Click-iT™ azide handle (Figure 2).

The Click-iT™ *O*-GlcNAc Enzymatic Labeling System supplies the key reagents for *in vitro* labeling of *O*-GlcNAc–modified glycoproteins. The →

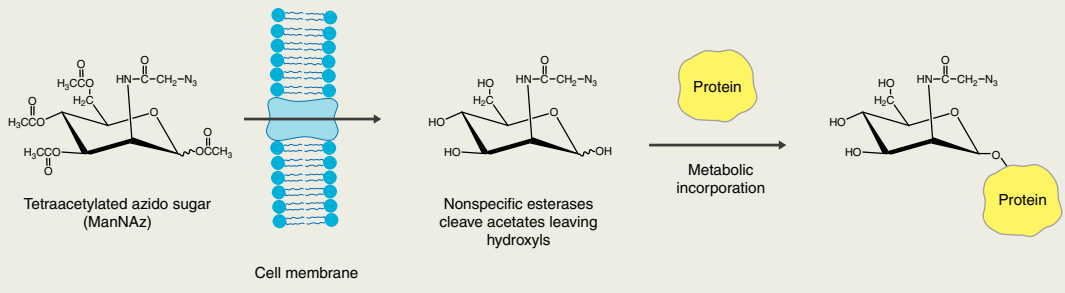

Figure 2—Metabolic incorporation of tetraacetylated azido sugars.

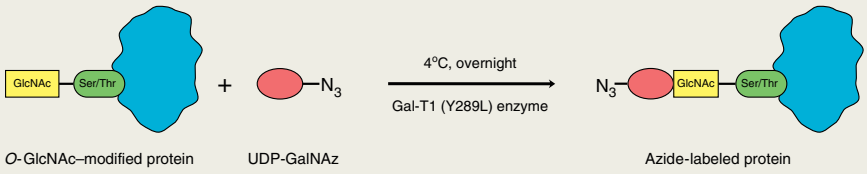

Figure 3—Enzymatic labeling of an *O*-GlcNAc–modified glycoprotein with UDP-GalNAz and the permissive mutant β-1,4-galactosyltransferase (Gal-T1 (Y289L)).

O-GlcNAc modification is a highly dynamic, intracellular regulatory modification found in all eukaryotic cells and, like phosphorylation, significantly alters target protein function.[9–12] *O*-GlcNAc–modified glycoproteins are enzymatically labeled with the Click-iT™ azide handle by utilizing the permissive mutant β-1,4-galactosyltransferase (Gal-T1 (Y289L)), which transfers azide-modified galactosamine (GalNAz) from UDP-GalNAz to *O*-GlcNAc residues on the target proteins[10] (Figure 3).

When it's time to detect the Click-iT™ azide handle, you have a choice of three different Click-iT™ Glycoprotein Detection Kits (Table 2), which provide either a fluorescent or biotinylated azide-reactive alkyne along with the critical click reaction components:

- Click-iT™ Tetramethylrhodamine (TAMRA) Glycoprotein Detection Kit
- Click-iT™ Dapoxyl® Glycoprotein Detection Kit
- Click-iT™ Biotin Glycoprotein Detection Kit

Glycoproteins labeled with a fluorescent alkyne can be directly detected in 1D or 2D gels using the appropriate excitation sources (300 nm UV illumination or 532 nm laser for the TAMRA fluorophore, 300 or 365 nm UV illumination for the Dapoxyl® fluorophore). Their spectral compatibility with total-protein, glycoprotein, and phosphoprotein gel stains is shown in Table 2. Glycoproteins labeled with the biotin alkyne can be detected on a western blot before or after probing with a primary antibody. In 1D gels and western blots, Click-iT™ technology enables the detection of a few hundred femtomoles of glycoprotein, allowing an in-depth analysis of glycosylation and its elusive cellular functions that was previously unattainable with conventional glycan labeling tools.

Publish—Truly comprehensive protein glycosylation analyses

One key advantage of the Click-iT™ method is the potential to multiplex with other detection technologies, permitting an unprecedented characterization of cellular posttranslational modifications. Used in combination with Multiplexed Proteomics® technologies, Click-iT™ labeling and detection reagents allow researchers to detect specific glycosylation subclasses together with total protein, total glycoproteins, or total phosphoproteins—all in the same gel (Table 2). With unsurpassed sensitivity over antibody-based detection methods (Figure 4), the Click-iT™ products provide a means of detecting low-abundance glycoproteins as well as glycoproteins with a small degree of glycosylation. This sensitivity may be a critical factor when analyzing the relationship between the *O*-GlcNAc modification and phosphorylation of Ser/Thr residues on key regulatory proteins.[10,13]

Table 2—Compatibility of the Click-iT™ Glycoprotein Detection Kits.

		Compatibility with detection methods			Spectral compatibility with Multiplexed Proteomics® stains		
Click-iT™ Glycoprotein Detection Kit	Cat. no.	1D or 2D gel	Western blot	Mass spectrometry	SYPRO® Ruby protein gel stain	Pro-Q® Emerald glycoprotein gel stain	Pro-Q® Diamond phosphoprotein gel stain
Click-iT™ Tetramethylrhodamine (TAMRA) Glycoprotein Detection Kit	C33370	●	●	●	●	●	
Click-iT™ Dapoxyl® Glycoprotein Detection Kit	C33371	●		●	●		●
Click-iT™ Biotin Glycoprotein Detection Kit	C33372		●	●			

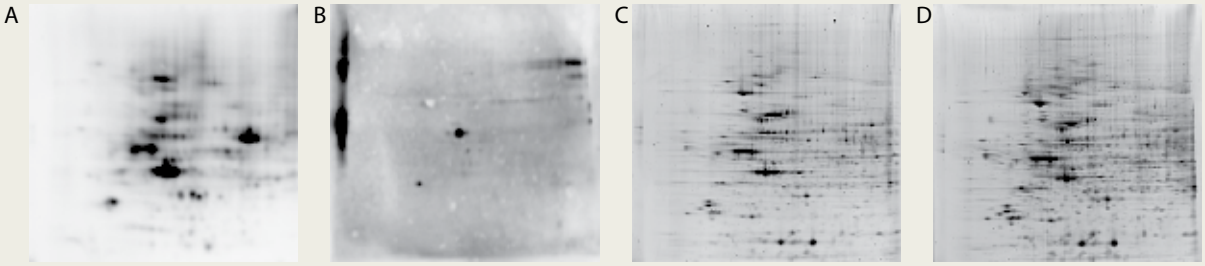

Figure 4—Comparison of Click-iT™ metabolic detection of *O*-GlcNAc–modified glycoproteins with antibody-based detection. (A) Jurkat cells were metabolically labeled with Click-iT™ GlcNAz metabolic glycoprotein labeling reagent, followed by biotinylation of the GlcNAz-labeled proteins with the Click-iT™ Biotin Glycoprotein Detection Kit. 20 mg of cell extract was separated on pH 4–7 IEF strips followed by NuPAGE® gel electrophoresis, then blotted to PVDF membrane. Biotinylated *O*-GlcNAc glycoproteins were visualized with streptavidin–horseradish peroxidase (HRP). (B) 2D western blot of 40 mg unlabeled Jurkat cell extract separated and blotted as in (A), then visualized with the anti–*O*-GlcNAc antibody CTD110.6, followed by the HRP conjugate of goat anti–mouse IgG antibody. In (A) and (B) HRP detection was performed using the protocols and reagents provided in the Pierce *O*-GlcNAc detection kit. The marker lane on the left in (B) contains 5 ng of the *O*-GlcNAc bovine serum albumin (BSA) positive control from the Pierce kit. (C) Gel of sample (A) stained with SYPRO® Ruby total protein stain. (D) Gel of sample (B) stained with SYPRO® Ruby total protein stain.

Finally, glycoproteins labeled with the Click-iT™ labeling and detection reagents are completely compatible with downstream LC-MS/MS and MALDI-MS analyses for further identification and characterization. For added convenience, we offer an *O*-GlcNAc peptide LC/MS standard (C33374) from the transcription factor CREB for LC-MS/MS and MALDI-MS analyses of the *O*-GlcNAc posttranslational modification. This peptide is also available together with its phosphorylated counterpart for use as LC/MS standards (C33373) in differential mass spectrometry–based studies of the corresponding modifications, as well as for characterizing differential β-elimination/addition conditions.

If you have questions about the Click-iT™ technology or would like to suggest ideas for the next Click-iT™ products, please send us an email at **reactions@invitrogen.com**. ■

References

1. Breinbauer, R. and Köhn, M. (2003) *ChemBioChem* 4:1147–1149.
2. Wang, Q. et al. (2003) *J Am Chem Soc* 125:3192–3193.
3. Rostovtsev, V.V. (2002) *Angew Chem Int Ed Engl* 41:2596–2599.
4. Kolb, H.C. et al. (2001) *Angew Chem Int Ed Engl* 40:2004–2021.
5. Sawa, M. et al. (2006) *Proc Natl Acad Sci U S A* 103:12371–12376.
6. Dube, D.H. et al. (2006) *Proc Natl Acad Sci U S A* 103:4819–4824.
7. Prescher, J.A. et al. (2004) *Nature* 430: 873–877.
8. Luchansky, S.J. et al. (2003) *Methods Enzymol* 362:249–272.
9. Saxon, E. and Bertozzi, C.R. (2000) *Science* 287:2007–2010.
10. Love, D.C. and Hanover, J.A. (2005) *Sci STKE* 2005:re13.
11. Ramakrishnan B. and Qasba P.K. (2002) *J Biol Chem* 277:20833–20839.
12. Khidekel, N. et al. (2003) *J Am Chem Soc* 125:16162–16163.
13. Slawson, C. (2006) *J Cell Biochem* 97:71–83.

Product	Quantity	Cat. no.
Click-iT™ GalNAz metabolic glycoprotein labeling reagent (tetraacetylated *N*-azidoacetylgalactosamine) *for *O*-linked glycoproteins* *5.2 mg*	1 each	C33365
Click-iT™ GlcNAz metabolic glycoprotein labeling reagent (tetraacetylated *N*-azidoacetylglucosamine) *for *O*-GlcNAc-modified proteins* *5.2 mg*	1 each	C33367
Click-iT™ ManNAz metabolic glycoprotein labeling reagent (tetraacetylated *N*-azidoacetyl-D-mannosamine) *for sialic acid glycoproteins* *5.2 mg*	1 each	C33366
Click-iT™ *O*-GlcNAc Enzymatic Labeling System *for *O*-linked GlcNAc glycoproteins* *10 labelings*	1 kit	C33368
Click-iT™ Biotin Glycoprotein Detection Kit *10 reactions*	1 kit	C33372
Click-iT™ Dapoxyl® Glycoprotein Detection Kit *for UV excitation* *10 reactions*	1 kit	C33371
Click-iT™ Tetramethylrhodamine (TAMRA) Glycoprotein Detection Kit *UV/532 nm excitation* *10 reactions*	1 kit	C33370
Click-iT™ *O*-GlcNAc peptide and phosphopeptide LC/MS standards *5 nmol each*	1 set	C33373
Click-iT™ *O*-GlcNAc peptide LC/MS standard (H-Thr-Ala-Pro-Thr-(*O*-GlcNAc)Ser-Thr-Ile-Ala-Pro-Gly-OH) *Theoretical Mass (M+H): 1118.50*	5 nmol	C33374

Optimally labeled fluorescent antibodies for *in vivo* animal imaging

SAIVI™ ALEXA FLUOR® ANTIBODY/PROTEIN LABELING KITS.

Stringent labeling requirements for *in vivo* animal imaging applications

The optimal fluorescent antibody conjugate for *in vitro* detection assays produces an intense fluorescent signal yet retains the binding selectivity and kinetics of the unlabeled antibody. When preparing a fluorescent antibody conjugate for *in vivo* animal imaging, however, the pharmacokinetics of the labeled probe must also be considered. In both *in vitro* and *in vivo* applications, a more heavily labeled antibody does not usually produce a better conjugate. Antibody conjugates with a very high degree of labeling (DOL) typically precipitate out of solution, bind nonspecifically, or exhibit intramolecular fluorescence quenching, making it necessary to have a less-than-maximal DOL to obtain a functional fluorescent antibody. For *in vivo* labeling experiments, the DOL of an antibody conjugate is even more severely restricted because it has significant consequences for the biodistribution and clearance of the probe. These additional constraints have led us to investigate the effects of DOL on fluorescent antibody conjugates used for *in vivo* animal imaging.

Effects of DOL on pharmacokinetics of fluorescent antibodies

To examine the pharmacokinetics of fluorescent antibodies with different DOL, we labeled anti-CEA (carcinoembryonic antigen) antibody at 1.1, 2.4, 3.9, and 6.0 dyes per antibody using the SAIVI™ Alexa Fluor® 750 Antibody/Protein Labeling Kit, which is specifically designed for creating azide-free antibody conjugates for injection. These fluorescent antibody conjugates were then injected intravenously into mice bearing LS174-T human tumor xenografts and imaged at varying times postinjection. As seen in Figure 1, the xenograft was most clearly detected using the fluorescent antibody with a DOL of 2.4. When imaged ventrally, these same mice exhibited nonspecific liver fluorescence that was more intense as the DOL of the antibody conjugates increased (Figure 2), suggesting an antibody clearance mechanism mediated by the liver.

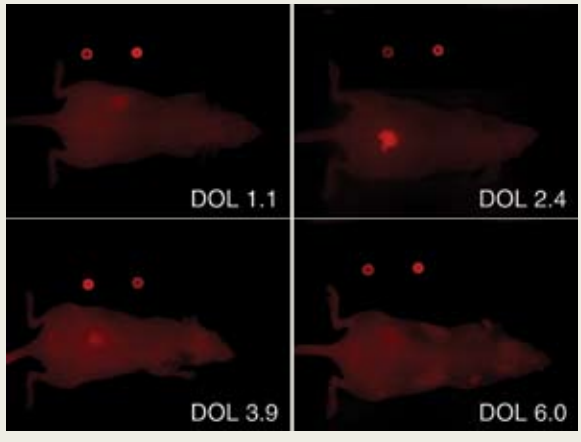

Figure 1—The fluorescence intensity of *in vivo* xenograft target labeling is not proportional to the degree of labeling (DOL) of the antibody conjugate. Anti-CEA (carcinoembryonic antigen) antibody (Zymed® Col-1 clone) was labeled with Alexa Fluor® 750 dye at different DOL (1.1, 2.4, 3.9, and 6.0) using the SAIVI™ Alexa Fluor® 750 Antibody/Protein Labeling Kit. Fifty micrograms of each of these fluorescent anti-CEA conjugates was then injected intravenously via the tail vein of athymic nude (nu/nu) mice carrying LS174-T (ATCC) human colon cancer xenografts of similar size. At 24 hours postinjection, the mice were imaged dorsally using an excitation wavelength of 735 nm and an emission range of 790–950 nm on the Maestro™ In-Vivo Imaging System (Cambridge Research & Instrumentation). The image cubes were spectrally processed using the Maestro™ software, which uses multispectral imaging technology to spectrally isolate the Alexa Fluor® 750 emission from autofluorescence in a defined area, and then quantitates it. As shown here, increasing the DOL of the fluorescent antibody above the optimal level caused a decrease in signal intensity. The two fluorescent dots at the top of each image were placed directly on the stage at the time of image collection to control for intensity levels.

This effect of DOL on pharmacokinetics is not limited to anti-CEA antibody conjugated to Alexa Fluor® 750 dye. We have observed similar results with anti-CEA antibody conjugated to Alexa Fluor® 680 dye, as well as with anti-EGFR (epidermal growth factor receptor) antibody conjugated to either Alexa Fluor® 680 dye or Alexa Fluor® 750 dye (Figure 3). The SAIVI™ Alexa Fluor® Antibody/Protein Labeling Kits—available with a choice of three different near-IR–emitting Alexa Fluor® dyes—provide a convenient method for preparing fluorescent antibody conjugates while carefully controlling the labeling using the DOL modulating reagent. By enabling you to quickly and reproducibly label and purify antibody conjugates with varying ratios of dye to protein, these kits allow you to optimize the fluorescence labeling in your *in vivo* imaging experiments. ■

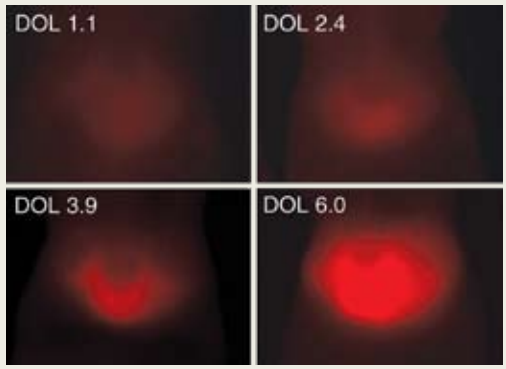

Figure 2—The fluorescence intensity of *in vivo* liver accumulation increases as the degree of labeling (DOL) of the antibody conjugate increases. The same mice shown in Figure 1 were also imaged ventrally using an excitation wavelength of 735 nm and an emission range of 790–950 nm on the Maestro™ In-Vivo Imaging System (Cambridge Research & Instrumentation). As the DOL of the fluorescent antibody increased, the signal intensity in the liver region also increased. At higher than optimal DOL, the intensity of the liver signal was greater than the intensity of the xenograft target signal (data not shown).

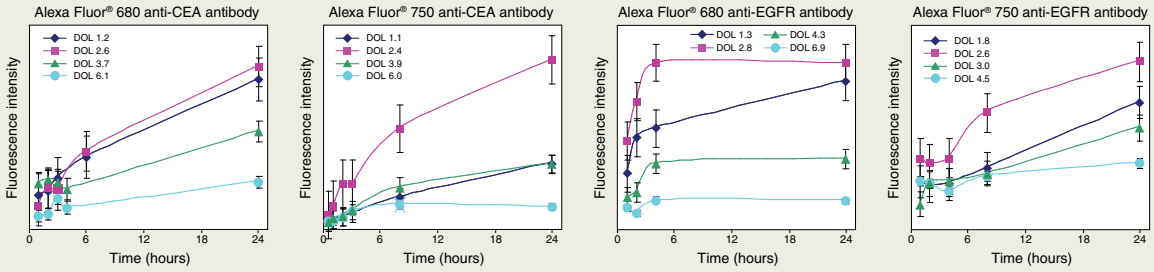

Figure 3—The fluorescence intensity of *in vivo* xenograft target labeling varies with degree of labeling (DOL) of the antibody conjugate. Two monoclonal mouse antibodies—the anti-CEA (carcinoembryonic antigen) antibody (Zymed® Col-1 clone) and the anti-EGFR (epidermal growth factor receptor) antibody (Zymed® 31G7 clone)—were conjugated to either Alexa Fluor® 680 or Alexa Fluor® 750 dyes at varying DOL using the SAIVI™ Alexa Fluor® Antibody/Protein Labeling Kits, injected into xenograft-bearing mice, and then imaged at various time points using the Maestro™ In-Vivo Imaging System (Cambridge Research & Instrumentation). In these examples, the fluorescent antibodies that produced the highest fluorescence intensity at the xenograft site had a DOL between 2 and 3.

Product	Quantity	Cat. no.
SAIVI™ Alexa Fluor® 647 Antibody/Protein 1 mg Labeling Kit *3 labelings*	1 kit	S30044
SAIVI™ Alexa Fluor® 647 Antibody/Protein 0.1 mg Labeling Kit *5 labelings*	1 kit	S30043
SAIVI™ Alexa Fluor® 680 Antibody/Protein 1 mg Labeling Kit *3 labelings*	1 kit	S30039
SAIVI™ Alexa Fluor® 680 Antibody/Protein 0.1 mg Labeling Kit *5 labelings*	1 kit	S30041
SAIVI™ Alexa Fluor® 750 Antibody/Protein 1 mg Labeling Kit *3 labelings*	1 kit	S30040
SAIVI™ Alexa Fluor® 750 Antibody/Protein 0.1 mg Labeling Kit *5 labelings*	1 kit	S30042

FROM A STEM CELL PERSPECTIVE

The technical challenges of working with stem cells can be daunting. Whether you are maintaining a population of undifferentiated stem cells or examining a specific differentiation pathway, the fast-paced arena of stem cell research relies on constantly adapting and improving the available cell biology tools. In this group of articles, we describe three fluorescence-based cell biology probes and their application to stem cell research. The Qtracker® Cell Labeling Kits are useful for labeling and subsequently separating feeder cells from stem cells by flow cytometry. The ELF® 97 Endogenous Phosphatase Detection Kit provides a simple method for monitoring alkaline phosphatase activity, a key marker of undifferentiated stem cells. And the LipidTOX™ neutral lipid stains selectively label neutral lipids in cells, enabling real-time detection and quantitation of adipogenesis. While these fluorescent probes have little in common structurally or mechanistically, they each have been shown to effectively address a specific facet of stem cell research.

Sorting out feeder cells co-cultured with embryonic stem cells

IDENTIFY AND SEPARATE INDIVIDUAL CELL TYPES USING QTRACKER® CELL LABELING KITS.

Technical barrier: Separating stem cells from their feeder cells

Human embryonic stem (hES) cells require culture under conditions that prevent differentiation. To maintain their potency, hES cells are commonly co-cultured with mitotically inactive mouse embryonic fibroblasts (MEF) as feeder cells. This practice, however, presents challenges to the subsequent physical isolation of hES cells, where MEF contamination is not desired. An effective cell separation strategy would utilize a long-lasting live-cell label that does not compromise viability yet provides a detectable handle for subsequent identification and isolation of labeled cells before or after fixation.

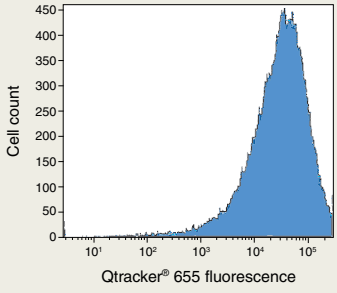

Figure 1—Flow cytometric analysis of mouse embryonic fibroblasts labeled with the Qtracker® 655 Cell Labeling Kit. Mitotically inactive mouse embryonic fibroblasts (MEF) were cultured for 48 hours and then labeled with the Qtracker® 655 Cell Labeling Kit. This FACS histogram illustrates that 97% of the MEF were labeled with the Qdot® 655 nanocrystals.

Solution: Labeling feeder cells with Qdot® nanocrystals

Qtracker® Cell Labeling Kits provide a simple and efficient method for fluorescently labeling MEF feeder cells with Qdot® nanocrystals, allowing straightforward identification and isolation of these cells in an hES cell co-culture. To gain access to the cytoplasm, the Qdot® reagents supplied in these kits employ a selective targeting peptide noncovalently bound to the fluorescent nanocrystal. Once internalized by the cell via endocytosis, the Qdot® nanocrystals exhibit intense, photostable fluorescence that can be observed using continuous illumination without time constraints due to photobleaching or degradation. The Qdot® nanocrystals are distributed in vesicles throughout the cytoplasm, can be observed up to five weeks after labeling, and are not transferred to adjacent cells in the population. Moreover, experiments indicate that Qtracker® labeling does not significantly affect cell viability or cellular enzyme activity.

We have demonstrated the utility of this cell separation strategy by labeling MEF using the Qtracker® 655 Cell Labeling Kit and then culturing these feeder cells with either SA2p12 hES cells or BG1vp22 hES cells. Our analysis of MEF labeled with Qdot® 655 nanocrystals by flow

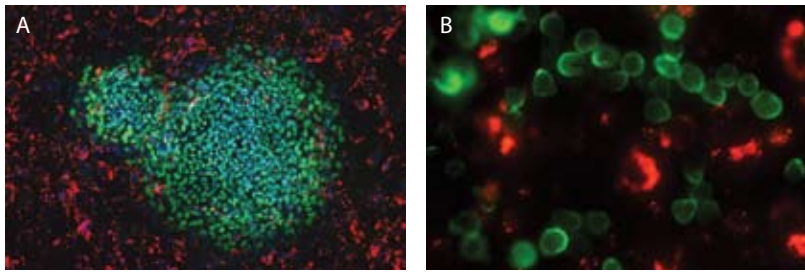

Figure 2—Immunocytochemical analysis of human embryonic stem (hES) cells co-cultured with mouse embryonic fibroblasts (MEF). BG1vp22 and SA2p12 hES cells were each plated onto a Qdot® 655 nanocrystal–labeled MEF feeder layer and allowed to grow for 48 hours. The cells were then fixed, labeled with anti-Oct4 or anti–Tra-1-81 primary antibody and green-fluorescent Alexa Fluor® 488 secondary antibodies, and analyzed by fluorescence microscopy. Micrograph A shows a colony of Oct4-expressing BG1vp22 cells (green) co-cultured with Qdot® 655 nanocrystal–labeled MEF (red) and counterstained with DAPI (blue). Micrograph B shows a suspension of Tra-1-81–expressing SA2p12 cells (green) co-cultured with Qdot® 655 nanocrystal–labeled MEF (red).

cytometry shows a labeling efficiency of 97% using the reagents and standard protocol provided by the kit (Figure 1). After co-culturing the labeled MEF with hES cells for 48 hours, the cell preparations were fixed and subjected to immunocytochemical analysis using primary antibodies specific for hES cell markers and secondary antibodies labeled with the green-fluorescent Alexa Fluor® 488 dye. For all markers tested, the labeled MEF were easily discriminated from colonies of BG1vp22 hES cells (Figure 2A) and from suspensions of SA2p12 hES cells (Figure 2B) using fluorescence microscopy. In fact, the hES cells appeared to exclude the feeder cells rather than grow on top of them. Furthermore, we obtained a clean separation of antibody-labeled hES cells and Qdot® 655 nanocrystal–labeled MEF by flow cytometry, with very little overlap of the two populations and no double staining observed in any of the cells (Figure 3).

These findings illustrate the usefulness of Qtracker® Cell Labeling Kits for labeling live feeder cells and subsequently separating them from co-cultured hES cells. Qtracker® Cell Labeling Kits are available containing Qdot® nanocrystals in one of seven brilliant fluorescent colors (525 nm, 565 nm, 585 nm, 605 nm, 655 nm, 705 nm, or 800 nm emission) and can be used together for multiplexing applications. ■

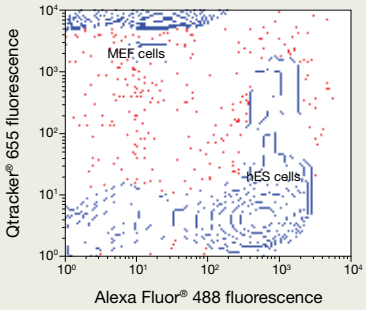

Figure 3—Flow cytometric analysis of human embryonic stem cells and mouse embryonic fibroblasts. Human embryonic stem (hES) cells, co-cultured with Qtracker® 655 nanocrystal–labeled mouse embryonic fibroblasts (MEF), were labeled with anti-SSEA4 primary antibody and Alexa Fluor® 488 secondary antibody. The cells were then analyzed by flow cytometry using 488 nm excitation. This contour plot, gated on cells by scatter, shows Alexa Fluor® 488 fluorescence vs. Qtracker® 655 fluorescence. The cultured hES cells show both positive and negative populations for SSEA-4 expression and have low fluorescence in the Qtracker® 655 channel. The MEF cells are so much brighter than the hES cells in the Qtracker® channel that both populations could not be on scale at the same time. This population resolution allows for easy discrimination or sorting of MEF from hES cells.

Multiplexing your panel of embryonic stem cell markers

LABEL UNDIFFERENTIATED CELLS USING ELF® 97 ALKALINE PHOSPHATASE SUBSTRATE.

Technical barrier: Finding compatible labels for multiplex assays

Endogenous alkaline phosphatase expression is a well-established marker for undifferentiated embryonic stem cells. In this specialized application, however, traditional histological methods for alkaline phosphatase fall short. Colorimetric and fluorometric reagents, including the fast red violet dye, can generate high background signals and poor resolution. More importantly, these traditional histochemical stains are generally not amenable to assays designed for detecting the expression of multiple markers in a single cell preparation. An alkaline phosphatase–selective stain that can be multiplexed with other embryonic stem cell markers would provide significant advantages, not only for the characterization of embryonic stem cell lines, but also for the general investigation of the role of alkaline phosphatase in embryonic, developmental, and pathological pathways. →

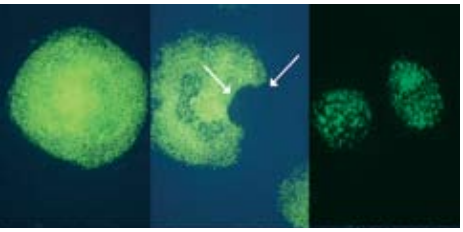

Figure 4—Human embryonic stem cells labeled with ELF® 97 alkaline phosphatase substrate. BG01V human embryonic stem (hES) cells (ATCC® SCRC-2002™) surrounded by feeder cells are fully undifferentiated, as evidenced by the presence of continuous green ELF® 97 fluorescence throughout the cell mass (left). While most of this BG01V colony remains undifferentiated, a locus of cells has differentiated, as shown by the lack of ELF® 97 fluorescence in one region (middle, arrows). The uneven green ELF® 97 fluorescence in these R1/E mouse embryonic stem cells (ATCC® SCRC-1036™) indicates nonuniform maintenance of the undifferentiated state (right). Images contributed by the American Type Culture Collection (ATCC®).

Solution: Multiplexing stem cell markers with ELF® 97 phosphate

ELF® 97 phosphate is a state-of-the-art fluorogenic phosphatase substrate that exhibits several key attributes for alkaline phosphatase localization in cells and tissues. Upon enzymatic cleavage, this weakly blue-fluorescent substrate yields a bright yellow-green–fluorescent precipitate with an unusually large Stokes shift and extremely photostable fluorescence (up to 500 times the photostability of fluorescein). These unique spectral characteristics make ELF® 97 phosphate optimally suited for multiparameter fluorescence assays.

Because the fluorescence excitation and emission maxima of the ELF® 97 precipitate (365/530 nm) are well separated, you can easily resolve the ELF® 97 signal from autofluorescence as well as from the signals of fluorescent antibody conjugates, binding proteins, and cellular counterstains. For example, ELF® 97 fluorescence emission can be clearly distinguished from that of the green-fluorescent Alexa Fluor® 488 dye by fluorescence microscopy using a standard DAPI longpass filter.

Furthermore, most phosphatase substrates used in histochemistry yield colorless, soluble hydrolysis products that must be coupled with a capture reagent to generate a colored or fluorescent precipitate. In contrast, hydrolysis of ELF® 97 phosphate generates a fluorescent precipitate at the site of enzymatic activity, which not only leads to higher resolution and lower background but also significantly reduces the amount of time required for detection.

Because endogenous alkaline phosphatase expression is a well-established marker for undifferentiated embryonic stem cells, Plaia and coworkers recently reported the use of the versatile ELF® 97 Endogenous Phosphatase Detection Kit to characterize a new variant human embryonic stem cell line, BG01V[1] (Figure 4). ELF® 97 phosphate was found to be so useful in this application that ATCC® (American Type Culture Collection) licensed the ELF® 97 technology and developed an optimized protocol and kit specifically designed for embryonic stem cell applications. The ATCC® ELF® Phosphatase Detection Kit (cat. no. SCRR-3010, www.atcc.org) is easy to use and signal development is very rapid, usually only 30–90 seconds. ■

Following differentiation into adipocytes

STUDY ADIPOGENESIS USING LIPIDTOX™ NEUTRAL LIPID STAINS.

Technical barrier: Selectively detecting neutral lipids

Adipogenesis, or the differentiation of preadipocytes into fat cells, provides a window into the complex sequence of events that directs multipotent progenitors to undergo phenotypic changes upon differentiation.[2] Implicated in several diseases including obesity, atherosclerosis, and steatosis,[3] the adipogenic pathway is actively studied using cellular models such as mouse 3T3-L1 fibroblasts and human mesenchymal stem cells in order to better understand and regulate this process.

Nile red, the standard reagent for monitoring neutral lipid accumulation during adipogenesis,[4] has significant drawbacks in this application. Importantly, nile red is not a specific stain for neutral lipids because it also stains phospholipids. Moreover, the fluorescence emission spectrum of nile red is quite broad, spanning the green (FITC) and red (TRITC) channels and complicating multiparametric studies. A neutral lipid–specific fluorescent stain with a narrow emission spectrum would allow researchers to better target the accumulation of fat droplets during adipogenesis and to combine this labeling with other cell markers.

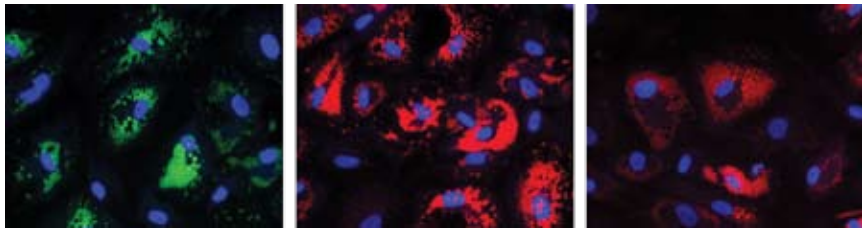

Figure 5—LipidTOX™ neutral lipid staining of lipid droplets in adipocytes. Adipocytes differentiated from human mesenchymal stem cells were fixed with formaldehyde and then stained with LipidTOX™ Green (excitation/emission ~495/505 nm) (left), LipidTOX™ Red (excitation/emission ~577/609 nm) (middle), and LipidTOX™ Deep Red (excitation/emission ~637/655 nm) (right) neutral lipid stains (green, bright red, and dark red lipid droplets, respectively); nuclei were counterstained with DAPI (blue).

Solution: Examining adipogenesis with LipidTOX™ neutral lipid stains

Originally developed for high content screening (HCS)–based cytotoxicity assays, LipidTOX™ neutral lipid stains are very useful for studying adipogenesis. Now available as stand-alone reagents, LipidTOX™ neutral lipid stains provide a simple, rapid, and specific method for staining neutral lipids in live or fixed cells. These neutral lipid–specific fluorescent dyes—available with narrow green, red, or far-red emission (Figure 5)—are supplied as ready-to-use formulations for easy setup, and require no sonication or organic solvents before use nor wash steps prior to imaging. Furthermore, the LipidTOX™ neutral lipid stains are readily incorporated into standard cell labeling procedures, including immunocytochemistry protocols, provided that detergents such as saponin or digitonin are used for cell permeabilization (Figure 6).

LipidTOX™ Green, Red, and Deep Red neutral lipid stains have been validated in studies with cells undergoing adipogenesis, as well as in cytotoxicity assays with compounds known to cause steatosis. With their selective labeling and narrow fluorescence emissions, these LipidTOX™ stains provide researchers with the specificity and flexibility needed for multiparametric analysis in adipogenesis applications. The LipidTOX™ Green neutral lipid stain is also available as part of the HCS LipidTOX™ Phospholipidosis and Steatosis Detection Kit, which provides a complete set of reagents for performing image-based HCS assays to characterize the potentially toxic side effects of compounds on lipid metabolism in mammalian cell lines. ■

References

1. Plaia, T.W. et al. (2006) *Stem Cells* 24:531–546.
2. Rosen, E.D. and Spiegelman, B.M. (2000) *Annu Rev Cell Dev Biol* 16:145–171.
3. Gregoire, F.M. et al. (1998) *Physiol Rev* 78:783–809.
4. Greenspan, P. and Fowler, S.D. (1985) *J Lipid Res* 26:781–89.

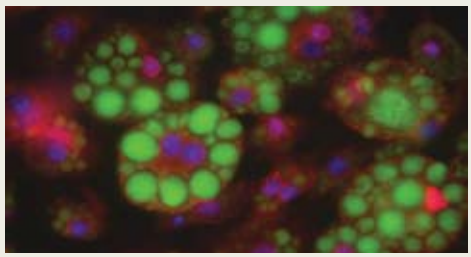

Figure 6—LipidTOX™ Green neutral lipid stain and fatty acid–binding protein (FABP4) antibody labeling in adipocytes. Adipocytes differentiated from 3T3-L1 mouse fibroblasts were fixed with formaldehyde and permeabilized with saponin before labeling with rabbit IgG anti–fatty acid binding protein (FABP4) antibody and Alexa Fluor® 594 goat anti–rabbit IgG antibody (red). These cells were then stained with LipidTOX™ Green neutral lipid stain (green), counterstained with DAPI (blue), and mounted in ProLong® Gold antifade mounting medium.

Product	Quantity	Cat. no.
Qtracker® 525 Cell Labeling Kit	1 kit	Q25041MP
Qtracker® 565 Cell Labeling Kit	1 kit	Q25031MP
Qtracker® 585 Cell Labeling Kit	1 kit	Q25011MP
Qtracker® 605 Cell Labeling Kit	1 kit	Q25001MP
Qtracker® 655 Cell Labeling Kit	1 kit	Q25021MP
Qtracker® 705 Cell Labeling Kit	1 kit	Q25061MP
Qtracker® 800 Cell Labeling Kit	1 kit	Q25071MP
ELF® 97 Endogenous Phosphatase Detection Kit	1 kit	E6601
ELF® spin filters *20 filters*	1 box	E6606

Product	Quantity	Cat. no.
HCS LipidTOX™ Green neutral lipid stain *solution in DMSO* *for cellular imaging*	each	H34475
HCS LipidTOX™ Red neutral lipid stain *solution in DMSO* *for cellular imaging*	each	H34476
HCS LipidTOX™ Deep Red neutral lipid stain *solution in DMSO* *for cellular imaging*	each	H34477
HCS LipidTOX™ Phospholipidosis and Steatosis Detection Kit *for high content screening* *for cellular imaging* *2-plate size*	1 kit	H34157
HCS LipidTOX™ Phospholipidosis and Steatosis Detection Kit *for high content screening* *for cellular imaging* *10-plate size*	1 kit	H34158

Multiparametric approaches for studying apoptosis

UNRAVELING THE SPATIAL AND TEMPORAL COMPONENTS OF PROGRAMMED CELL DEATH.

No single assay adequately characterizes apoptosis

The orderly progression toward cell death is fundamental to the life of a multicellular organism. Apoptosis—the genetically controlled ablation of cells—not only allows for proper growth and development by ridding the organism of unneeded cells and tissues, but also minimizes threats to the organism by destroying surplus cells of the immune system and virus-infected or DNA-damaged cells.[1,2]

Programmed cell death is morphologically and biochemically distinct from cell death by injury (necrosis). In contrast with necrotic cells, apoptotic cells exhibit compaction of the nuclear chromatin, shrinkage of the cytoplasm, and production of membrane-bound apoptotic bodies, as well as DNA fragmentation and cleavage or degradation of several cellular proteins. These differences can be selectively targeted with fluorescent probes in order to characterize the spatial and temporal components of apoptosis (Table 1). Incorrectly regulated apoptosis

Table 1—Temporal relationships of apoptotic events in Jurkat cells treated with camptothecin.

Time after induction	Cell function changes	Reagents used	Cat. no.
Early	Mitochondrial membrane potential	MitoTracker® Red CMXRos	M7512
		MitoProbe™ $DiOC_2(3)$ Assay Kit	M34150
		MitoProbe™ $DiIC_1(5)$ Assay Kit	M34151
		MitoProbe™ JC-1 Assay Kit	M34152
	Mitochondrial transition pore opening	Image-iT® LIVE Mitochondrial Transition Pore Assay Kit	I35103
		MitoProbe™ Transition Pore Assay Kit	M34153
	Phosphatidylserine translocation to outer membrane	Alexa Fluor® 488 annexin V	A13201
		Allophycocyanin (APC) annexin V	A35110
	Caspase activity	Image-iT® LIVE Green Caspase-3 and -7 Detection Kit	I35106
		Image-iT® LIVE Green Caspase-8 Detection Kit	I35105
		Image-iT® LIVE Green Poly Caspases Detection Kit	I35104
		Image-iT® LIVE Red Caspase-3 and -7 Detection Kit	I35102
		Image-iT® LIVE Red Poly Caspases Detection Kit	I35101
		Vybrant® FAM Caspase-3 and -7 Assay Kit	V35118
		Vybrant® FAM Caspase-8 Assay Kit	V35119
		Vybrant® FAM Poly Caspases Assay Kit	V35117
	Metabolic activity	Vybrant® Cell Metabolic Assay Kit	V23110
	DNA condensation	Vybrant® DyeCycle™ Violet stain	V35003
		Hoechst 33342	H1399, H3570
	DNA fragmentation	APO-BrdU™ TUNEL Assay Kit	A23210
		Anti-BrdU antibody	A21300, A21303
		Vybrant® DyeCycle™ Orange stain	V35005
Late	Plasma membrane integrity	Propidium iodide	P1304MP, P3566
		SYTOX® Green dye	S7020

PRODUCT HIGHLIGHT

Detection of sub-G_1 DNA peak

DNA fragmentation is a relatively late apoptotic event that follows chromatin condensation and is characterized by the appearance of a sub-G_1 population in apoptotic cells. This population is typically detected by flow cytometry using propidium iodide following cell permeabilization and extensive washing. We have found that a new cell-permeant DNA stain—Vybrant® DyeCycle™ Orange stain—can directly detect a sub-G_1 population in cells with intact plasma membranes. Vybrant® DyeCycle™ Orange stain was used to label Jurkat cells at time points up to 6 hours after treatment with camptothecin, and a reagent such as SYTOX® Red dead cell stain or SYTOX® Blue dead cell discriminator was used to exclude cells with damaged membranes. The sub-G_1 population was initially absent in intact cells (left panel) and first appeared at 3–4 hours post-induction, increasing with additional time of induction (right panel).

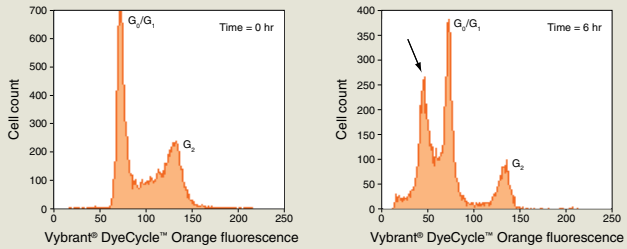

Multicolor staining using Vybrant® DyeCycle™ Orange stain and SYTOX® Red dead cell stain. Camptothecin-treated Jurkat cells were stained with 10 µM Vybrant® DyeCycle™ Orange stain, excited with 488 nm light, and 10 nM SYTOX® Red dead cell stain, excited with 633 nm light. Analysis was gated on cells with intact membranes using SYTOX® Red dead cell stain. These cells showed a distinct peak to the left of the G_0/G_1 peak after 6 hours of induction. The sub-G_1 population was confirmed as apoptotic by co-staining with 1 µM PO-PRO™-1 iodide.

Product	Quantity	Cat. no.
SYTOX® Blue dead cell stain *for flow cytometry* *1000 assays* *1 mM solution in DMSO*	1 ml	S34857
SYTOX® Red dead cell stain *for 633 or 635 nm excitation* *5 µM solution in DMSO*	1 ml	S34589
Vybrant® DyeCycle™ Orange stain *5 mM solution in DMSO* *200 assays*	400 µl	V35005

is implicated in a number of disease states, including cancer, stroke, Alzheimer's disease, and several autoimmune diseases,[3–5] making these probes important tools for understanding these pathways.

As with cell viability, no single parameter fully defines cell death in all systems. Therefore, it is often advantageous to use a multiparametric approach when studying apoptotic events and their temporal relationships. Here we summarize a series of Molecular Probes® reagents and assays for flow cytometry and fluorescence imaging analyses, as well as a diverse group of antibodies that recognize important apoptosis-related antigens (Tables 2 and 3). The Vybrant® Apoptosis Assay Kits provide a convenient means of detecting multiple apoptotic parameters in a single assay (Table 2). These probes enable you to distinguish live cells, apoptotic cells, and necrotic cells, as well as to determine the relative stage of apoptosis in your particular experimental system. For more information on our complete line of apoptosis products, please visit **probes.invitrogen.com/apoptosis**.

Table 2—Selected Vybrant® Apoptosis Assay Kits.

Kit name *	Vital cell stain	Apoptotic cell stain	Dead cell stain	Cell markers detected	Notes	Cat. no.
Vybrant® Apoptosis Assay Kit #2	NA	Alexa Fluor® 488 annexin V	Propidium iodide	Phosphatidylserine exposure and plasma membrane integrity	Two-color (green/red) assay for optimal separation of apoptotic and dead populations	V13241
Vybrant® Apoptosis Assay Kit #4	NA	YO-PRO®-1	Propidium iodide	Early loss of plasma membrane integrity	Two-color (green/red) assay for optimal separation of apoptotic and dead populations	V13243
Vybrant® Apoptosis Assay Kit #10	C_{12}-resazurin	Allophycocyanin annexin V	SYTOX® Green dye	Phosphatidylserine exposure, plasma membrane integrity, and cell vitality	Three-color (green/red/far-red) assay for optimal separation of viable, apoptotic, and dead populations	V35114
Vybrant® Apoptosis Assay Kit #11	MitoTracker® Red CMXRos	Alexa Fluor® 488 annexin V	NA	Phosphatidylserine exposure and mitochondrial membrane potential	Two-color (green/red) assay for optimal separation of viable and apoptotic populations	V35116
Vybrant® Apoptosis Assay Kit #12	NA	Vybrant® DyeCycle™ Violet stain	7-AAD	DNA fragmentation and membrane integrity	Two-color (blue/red) assay for optimal separation of apoptotic and dead populations	V35121

*For a complete list of Vybrant® Apoptosis Assay Kits, please visit **probes.invitrogen.com/apoptosis**. NA = not applicable; 7-AAD = 7-aminoactinomycin D.

Case in point: Multiparametric detection at work

Figure 1 illustrates how Molecular Probes® reagents and assay kits can be used for multiparametric analysis of apoptosis. We induced Jurkat cells with camptothecin and assayed over time for phosphatidylserine translocation to the outer membrane using fluorescent annexin V conjugates and for loss of membrane integrity using propidium iodide.[6] Flow cytometric analysis confirmed that the number of cells stained with green-fluorescent Alexa Fluor® 488 annexin V increased over time (green dots), while the number of cells stained with red-fluorescent propidium iodide remained relatively constant (blue dots) (Figure 1A, 1B, and 1C).

Table 3—Selected primary antibodies for studying apoptosis.

Target/ Antibody type	Clone/PAD	Western blotting	ELISA	Immuno-precipitation	Immuno-histochemistry	Immuno-fluorescence	Flow cytometry	Cat. no.
Annexin II—Specific for annexin II, and does not cross-react with other annexin proteins.								
Mouse IgG1	Z014	●	●		●			03-4400
ASPP2 (C-term)—Specific for ASPP2 (apoptosis-stimulating protein of p53 protein 2, p53-binding protein 2, 53BP2, Bcl2-binding protein (Bbp), PPP1R13A).								
Mouse IgG1 kappa	DX54.10	●	●	●		●		39-7000
BAG1—Specific for human BAG-1, BAG-1M, and BAG-1L proteins.								
Mouse IgG1 kappa	10B6H7	●	●	●	●	●		37-4000
Bax—Specific for the 21 kDa Bax protein.								
Mouse IgG1	2D2	●	●	●	●			33-6400, 18-0218
Mouse IgG1	6A7	●	●	●		●		33-6600
Bcl-2—Specific for the human Bcl-2 protein.								
Mouse IgG1 kappa	Bcl-2-100	●		●	●	●	●	13-8800, 18-0193Z
Bcl-XL—Specific for the Bcl-XL protein.								
Mouse IgG2a	2H12	●	●		●			33-6300, 18-0217
BrdU—Available unlabeled, as well as labeled with Alexa Fluor® 488, Alexa Fluor® 594, Alexa Fluor® 647, and Alexa Fluor® 680 dyes.								
Mouse IgG1 kappa	PRB-1				●	●	●	A21300, A21303, A21304, A21305, A31859
Caspase-3—Specific for human caspase-3.								
Mouse IgG2a	4-1-18	●			●			35-1600Z
Cytochrome *c*—Key component of the SelectFX® Alexa Fluor® 488 Cytochrome *c* Apoptosis Detection Kit.								
Mouse IgG					●	●		S35115
Lamin B1—Specific for the 68 kDa lamin B1 isoform; reactivity with other lamin isoforms has not been detected.								
Mouse IgG1 kappa	L-5	●	●	●		●		33-2000
Lamin B2—Specific for the 66 kDa lamin B2 isoform; reactivity with other lamin isoforms has not been detected.								
Mouse IgG1 kappa	E-3	●	●	●		●		33-2100
PARP—Specific for the 116 kDa full-length PARP protein, as well as its 85 kDa cleavage fragment. The immunoreactive epitope is contained within the C-terminal region of the 46 kDa DNA-binding domain of the PARP protein.								
Mouse IgG1 kappa	C-2-10	●	●			●		33-3100
RCAS1—Specific for the RCAS1 protein.								
Mouse IgG1 kappa	ZR001	●	●		●			39-2300
Smac/DIABLO—Specific for Smac/DIABLO, a 29 kDa mammalian mitochondrial protein that regulates apoptosis by binding apoptosis inhibitor proteins (IAPs).								
Mouse IgG1	17-1-87	●		●	●	●		35-6600

Using the Vybrant® FAM Poly Caspases Assay Kit in conjunction with fluorescent Alexa Fluor® 488 annexin V and propidium iodide probes, we could elucidate the temporal relationship between caspase activation, annexin binding, and loss of membrane integrity in identically induced Jurkat cells (Figure 1D, 1E, and 1F). The far-red–fluorescent allophycocyanin annexin V staining became prominent between 1 and 2 hours, while caspase activity increased after cells reacted with annexin V. Accordingly, cells with low caspase activity and increased annexin V binding were observed (arrow in Figure 1E). Similar results were seen with the Vybrant® FAM Caspase-3 and -7 Assay Kit and Vybrant® FAM Caspase-8 Assay Kit (data not shown), suggesting that phosphatidylserine translocation precedes caspase activation. A more detailed analysis of the temporal relationship of apoptotic events was obtained using additional probes, including MitoTracker® Red CMXRos and MitoProbe™ $DiIC_1(5)$ to detect changes in mitochondrial membrane potential, calcein to follow mitochondrial pore activation, and C_{12}-resazurin to monitor cell metabolism.[6] Multiparametric studies such as these can be used to determine the relative timing of apoptotic events and enable researchers to characterize specific apoptotic pathways. ■

References

1. Kerr, J.F. et al. (1972) *Br J Cancer* 26:239–257.
2. Ellis, R.E. et al. (1991) *Annu Rev Cell Biol* 7:663–698.
3. Meiler, J. and Schuler, M. (2006) *Curr Drug Targets* 7:1361–1369.
4. Ekshyyan, O. and Aw, T.Y. (2004) *Curr Neurovasc Res* 1:355–371.
5. Culmsee, C. and Landshamer, S. (2006) *Curr Alzheimer Res* 3:269–283.
6. Detection of Apoptosis Markers over Time after Induction (presented at The American Society for Cell Biology 44th Annual Meeting, Washington, DC; December 4–8, 2004).

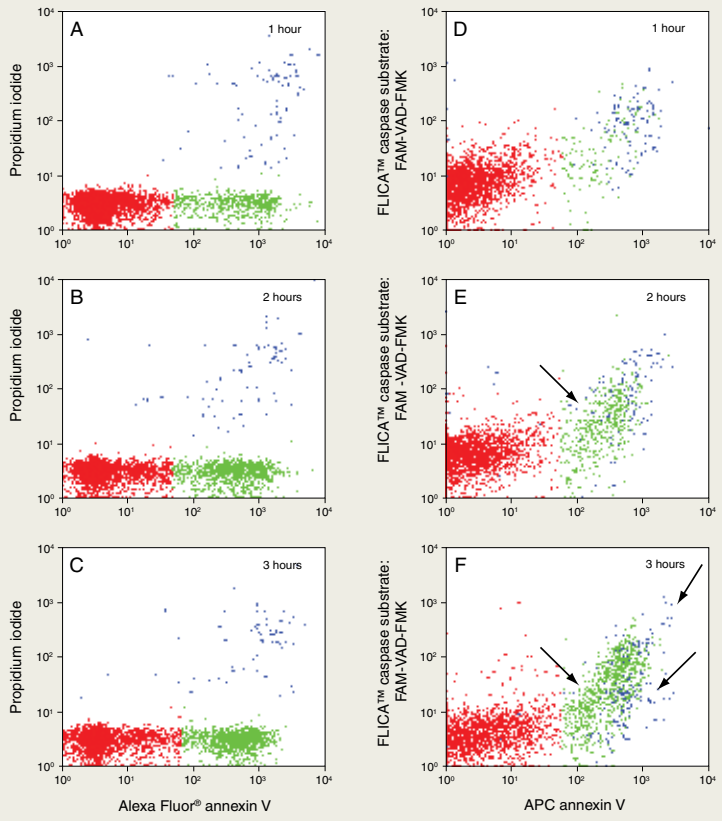

Figure 1—Flow cytometric analysis of multiple apoptotic events. Jurkat cells were treated with 10 µM camptothecin for 30 minutes to 3 hours to induce apoptosis, then stained with Alexa Fluor® 488 annexin V conjugate and propidium iodide (A, B, C) or with allophycocyanin (APC) annexin V conjugate, propidium iodide, and the FLICA™ caspase substrate FAM-VAD-FMK provided in the Vybrant® FAM Poly Caspases Assay Kit (D, E, F). The annexin V staining (indicating phosphatidylserine translocation to the outer membrane) became prominent between 1 and 2 hours, while caspase activity increased after the cells reacted with annexin V; cells with low caspase activity and increased annexin V binding are visible (arrow in Figure 1E). Cells stained with propidium iodide (indicating loss of membrane integrity) show both high and low polycaspase activity (arrows in Figure 1F). Blue dots represent propidium iodide–positive events (loss of membrane integrity); green dots represent annexin V–positive events (phosphatidylserine translocation); red dots represent live-cell events.

TC-FlAsH™ and TC-ReAsH™ reagents

LIVE-CELL IMAGING AND PROTEIN LABELING TOOLS.

The versatility of biarsenical reagents

Since Roger Tsien and colleagues first described the use of biarsenical reagents for the site-specific labeling of proteins in live cells in 1998, many applications for these reagents have been described in the literature (Table 1). Most applications describe the use of FlAsH and ReAsH reagents for labeling specific proteins in a live-cell context (references 1, 3–6, 8, 10–15) (Figure 1), while other publications describe the use of biarsenical technology in applications as varied as affinity purification, SDS-PAGE, and protease assays (references 2, 7, 9). Such extensive literature coverage indicates that FlAsH and ReAsH reagents represent a powerful and flexible labeling strategy for protein labeling.

How FlAsH and ReAsH work

The biarsenical labeling technology works through the high-affinity interaction of arsenic with thiols. The FlAsH reagent is essentially fluorescein that has been modified to contain two arsenic atoms at a set distance from each other (Figure 2A). Similarly, the ReAsH reagent is based on resorufin that has been modified to contain two appropriately spaced arsenic atoms. These virtually nonfluorescent reagents (shown in Figure 2B in an ethanedithiol (EDT)-bound state) become highly fluorescent upon binding to a tetracysteine (TC) sequence (Figure 3). The most commonly used TC sequence is the hexapeptide Cys-Cys-Pro-Gly-Cys-Cys; binding of the FlAsH or ReAsH reagent to this TC tag forms four covalent bonds, and the binding is reversible through competition with thiol-reducing agents. Thus, the method basically comprises incorporating a TC tag into a protein of interest, followed by detection with the green-fluorescent FlAsH or red-fluorescent ReAsH reagent.

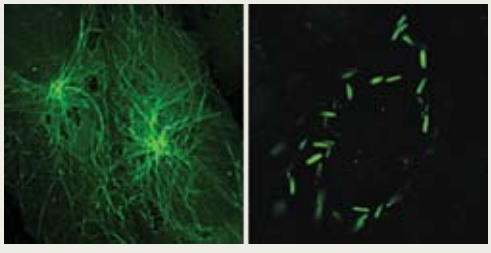

Figure 1—CHO-K1 cells expressing a tetracysteine-tagged version of β-tubulin labeled with TC-ReAsH™ reagent. Upon treatment with vinblastine, a compound known to perturb cytoskeletal structure, tubulin drastically rearranges from a reticular structure (A) to rod shaped (B).

One approach, many advantages

Several site-specific fluorescence tagging strategies have been developed for protein detection, including GFPs, Halo-tag, and SNAP-tag. Although fluorescent proteins remain the gold standard for live-cell imaging experiments due to their autofluorescent properties, exogenous fluorophore tagging strategies offer unique advantages. Using expression tags, researchers can add different fluorophores to change the color of a fusion protein, with no need to perform subcloning. Researchers can also base affinity purification strategies around the tag, attach nonfluorescent ligands such as biotin or a solid support, and utilize the tag for protein detection in SDS-PAGE (Figure 4).

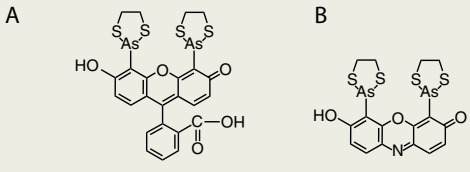

Figure 2—The structures of FlAsH-EDT$_2$ (A) and ReAsH-EDT$_2$ (B) biarsenical labeling reagents.

TC-FlAsH™ and TC-ReAsH™ reagents

Exemplifying the exogenous tagging method, Molecular Probes® TC-FlAsH™ and TC-ReAsH™ reagents are designed to provide optimum performance in the most challenging protein detection applications. Our TC-FlAsH™ and TC-ReAsH™ reagents encompass the full power of the technology, offering:

- a small tag size for minimal disruption of native protein structure/function
- very strong and reversible labeling
- extremely sensitive fluorogenic detection

For more information about these reagents and their use, visit our website at **probes.invitrogen.com**. ■

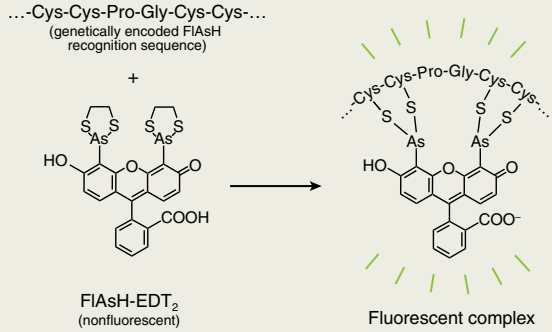

Figure 3—Schematic diagram of the fluorogenic nature of biarsenical reagents. Binding of the nonfluorescent FlAsH-EDT_2 reagent to a tetracysteine sequence yields a highly fluorescent complex.

Table 1—Publications describing unique applications of biarsenical reagents.

Year	Journal	Authors	Application	Reference
1998	*Science* 281:269	Griffin, B.A. et al.	Original description of FlAsH as a tool for site-specific labeling of proteins in live cells	1
2000	*Protein Sci* 9:213	Thorn, K.S. et al.	Affinity purification of TC-tagged proteins	2
2001	*Nat Biotechnol* 19:321	Rice, M.C. et al.	Experimental system for assessing gene repair using FlAsH in *Saccharomyces cerevisiae*	3
2002	*J Am Chem Soc* 124:6063	Adams, S.R. et al.	New blue and red biarsenical ligands	4
2002	*Science* 296:503	Gaietta, G. et al.	Correlation of electron microscopy to fluorescence microscopy	5
2003	*Nat Biotechnol* 21:1505	Tour, O. et al.	Genetically targeted chromophore-assisted light inactivation (CALI) using ReAsH	6
2004	*Electrophoresis* 25:2447	Feldman, G. et al.	In-gel detection of TC-tagged proteins using FlAsH	7
2004	*Nat Neurosci* 7:244	Ju, W. et al.	Pulse-chase experiments and trafficking of AMPA receptors using FlAsH and ReAsH	8
2005	*Anal Biochem* 336:75	Blommel, P.G.	Fluorescence anisotropy assay for protease activity of TC-tagged proteins	9
2005	*Nat Methods* 2:171	Hoffmann, C. et al.	A FlAsH-based FRET approach to determine GPCR activation in living cells	10
2005	*Nat Methods* 2:959	Enninga, J. et al.	Labeling of TC-tagged proteins in live bacteria	11
2005	*Nat Biotechnol* 23:1308	Martin, B.R. et al.	Optimization of the biarsenical-binding TC motif for mammalian cells	12
2006	*Biotechniques* 41:569	Estevez, J.M. and Somerville, C.	Live-cell imaging of synthetic peptides expressed in plants	13
2006	*J Am Chem Soc* 128:12040	Spagnuolo, C.C. et al.	Improved photostable FRET-competent TC probes	14
2006	*Nat Methods* 3:817	Arhel, N. et al.	Four-dimensional tracking of intracellular HIV complexes	15

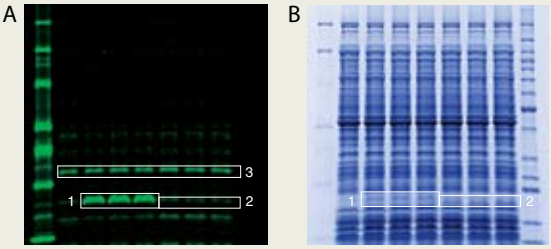

Figure 4—Protein detection using FlAsH reagent in polyacrylamide gels. FlAsH reagent was included in the sample loading buffer of TC-tagged acyl carrier protein (ACP) and untagged ACP in *E. coli* extract and subjected to SDS-PAGE. A fluorescent image was obtained directly after electrophoresis without the need for any gel staining or destaining (A). The gel was subsequently stained with SimplyBlue™ SafeStain and is shown for comparison (B). Box 1 highlights the TC-tagged ACP after 20, 60, and 180 minute *in vitro* protein synthesis reactions. Box 2 corresponds to untagged ACP. Box 3 is an endogenous *E. coli* protein that contains a naturally occurring tetracysteine sequence that allows FlAsH to bind.

Product	Quantity	Cat. no.
TC-FlAsH™ II In-cell Tetracysteine Tag Detection Kit *green fluorescence* *for live-cell imaging*	1 kit	T34561
TC-ReAsH™ II In-cell Tetracysteine Tag Detection Kit *red fluorescence* *for live-cell imaging*	1 kit	T34562
TC-FlAsH™ TC-ReAsH™ II In-cell Tetracysteine Tag Detection Kit *with mammalian TC-Tag Gateway® expression vectors* *green fluorescence* *red fluorescence*	1 kit	T34563

In situ hybridization made easy

FISH OR CISH? TWO WAYS TO VISUALIZE YOUR RNA AND DNA TARGETS *IN SITU*.

In situ hybridization (ISH) is a powerful technique for localizing specific nucleic acid targets within fixed tissues and cells, allowing you to obtain temporal and spatial information about gene expression and genetic loci. While the basic workflow of ISH is similar to that of blot hybridizations—the nucleic acid probe is synthesized, labeled, purified, and annealed with the specific target—the difference is the greater amount of information gained by visualizing the results within the tissue.

Today there are two basic ways to visualize your RNA and DNA targets *in situ*—fluorescence (FISH) and chromogenic (CISH) detection. Characteristics inherent in each method of detection (Table 1) have made FISH and CISH useful for very distinct applications. While both use a labeled, target-specific probe that is hybridized with the sample, the instrumentation used to visualize the samples is different for each method. Here we highlight the differences and the advantages of each method.

Table 1—Inherent characteristics of ISH methods.

Technique	Instrument/ visualization method	Primary advantage	Primary application
FISH	Epifluorescence or confocal microscope	Visualization of multiple targets in the same sample	Gene expression and cytogenetics
CISH	Bright-field microscope	Ability to view the CISH signal and tissue morphology simultaneously	Molecular pathology diagnostics

FISH for your gene expression studies

"Our lab routinely uses FISH, and the FISH Tag™ Kits offer us an unparalleled means for in-house generation of high-quality FISH probes. Their cost-effectiveness and flexibility, coupled with their ease of use, make FISH Tag™ Kits the ideal tool for diagnostic and research cytogenetics."

—Will Westra, The Scripps Research Institute, San Diego, CA

Multiplex fluorescence *in situ* hybridization (FISH) exemplifies the elegance that only fluorescence-based strategies offer: the ability to assay multiple targets simultaneously and visualize co-localization within a single specimen. Using spectrally distinct fluorophore labels for each different hybridization probe, this approach gives you the power to resolve several genetic elements or multiple gene expression patterns in a single specimen, with multicolor visual display.[1]

FISH Tag™ Detection Kits provide all of the tools you need—enzymes, purification technology, and brilliant Alexa Fluor® dye labeling—for generating optimal FISH probes for multiplex assays in just two steps.[2] Nick translation (for DNA probes) or *in vitro* transcription (for RNA probes) is used to enzymatically incorporate amine-modified nucleotides—aminoallyl dUTP for DNA or aminoallyl UTP for RNA—followed by chemical labeling with amine-reactive Alexa Fluor® dyes. Compared to dye-labeled nucleotides, aminoallyl-modified nucleotides are consistently incorporated at high levels and covalently labeled using reliable succinimidyl ester coupling chemistry. The end result

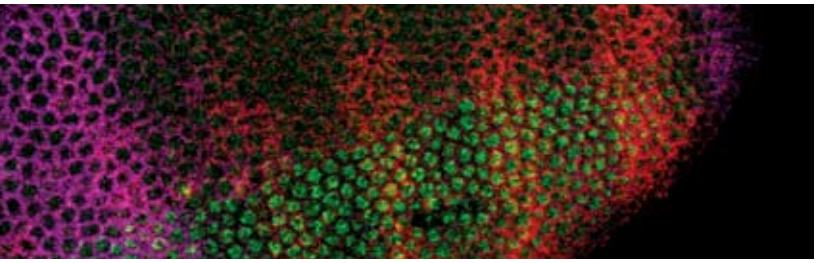

Figure 1—RNA targets labeled in a *Drosophila melanogaster* embryo. Simultaneous detection of expression of three genes in a whole mount *Drosophila melanogaster* embryo by fluorescence *in situ* hybridization (FISH) using the FISH Tag™ RNA Multicolor Kit. Green: *sog* (short gastrulation) labeled with Alexa Fluor® 488 dye; red: *ftz* (fushi tarazu) labeled with Alexa Fluor® 594 dye; magenta: *Kruppel* labeled with Alexa Fluor® 647 dye. The sample was mounted using *SlowFade®* Gold antifade reagent.

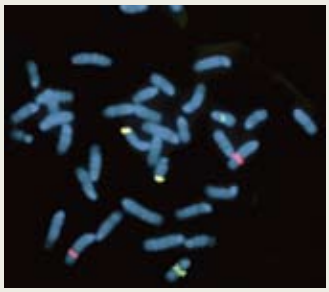

Figure 2—Mouse lymphocyte metaphase spread hybridized with locus-specific FISH probes labeled using FISH Tag™ Kits. Red: Chromosome 4 labeled with Alexa Fluor® 555 dye; yellow: Chromosome 10 labeled with Alexa Fluor® 647 dye (pseudocolored); green: Chromosome 16 labeled with Alexa Fluor® 488 dye. Image contributed by Will Westra, The Scripps Research Institute.

is a higher degree of labeling and improved signal-to-noise ratios in FISH applications. PureLink™ nucleic acid purification technology is included to rapidly and efficiently purify the labeled probe, providing high yields of DNA or RNA. *SlowFade®* Gold antifade reagent is included for superior photostability during imaging. And because there's no need for secondary detection, your results are immediate and visually distinct (Figures 1 and 2). FISH Tag™ Kits offer:

- a complete workflow solution for FISH applications
- exceptional signal intensity and photostability
- multiplexing capabilities with spectrally distinct dyes that allow you to view multiple targets simultaneously

In addition to the FISH Tag™ Kits, there are FISH labeling and detection options available for a variety of applications. For rare or very low-abundance targets, amplify the fluorescence signal of your FISH probes using the Alexa Fluor® dye tyramides in our TSA™ kits. Tyramide signal amplification (TSA) employs reliable horseradish peroxidase (HRP)–based signal amplification that is compatible with haptenylated probes such as those labeled with fluorescein, biotin, dinitrophenyl (DNP), or digoxigenin (Figure 3). In addition to the dramatic signal enhancement provided by TSA detection, dye tyramides are covalently deposited at the site of probe hybridization, providing excellent resolution and high signal-to-noise ratios. Alternatively, ARES™ DNA Labeling Kits provide two-step labeling technology in a basic kit format, without enzymes or a purification system. Protocols for nick translation and reverse transcription [2] are also included. In addition, the new ARES™ random priming protocol is optimized for generating bright FISH probes using this enzymatic labeling approach. ULYSIS™ Nucleic Acid Labeling Kits provide yet another option, offering direct, fast, and easy chemical labeling of nucleic acid probes. And ChromaTide® nucleotides include a variety of Alexa Fluor® and nonproprietary dye and haptenylated conjugates for synthesis of your probe for direct or indirect detection approaches. For a complete list of reagents and kits for your FISH applications, visit **probes.invitrogen.com**. →

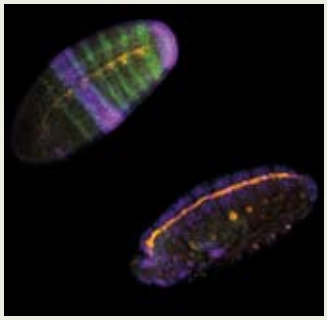

Figure 3—Advanced multiplexing capabilities achieved using a combination of FISH Tag™ and TSA™ Kits. *Drosophila melanogaster* embryos were hybridized with a green-fluorescent *ftz* probe (FISH Tag™ RNA Labeling Kit with Alexa Fluor® 488 dye), a far-red–fluorescent *Kruppel* probe (FISH Tag™ RNA Labeling Kit with Alexa Fluor® 647 dye), and a fluorescein UTP–labeled *Rhomboid* probe, followed by amplification of the probe signal with TSA™ technology using an anti-fluorescein/horseradish peroxidase (HRP) conjugate and Alexa Fluor® 555 tyramide (TSA™ Kit #40).

PRODUCT HIGHLIGHT

In situ hybridization system

In addition to reagents and kits for FISH and CISH, Invitrogen offers accessories and ancillary products such as the SPoT-Light® CISH™ Hybridizer, a hands-free denaturation and hybridization system. Note that the SPoT-Light® Hybridizer can be used with both FISH and CISH techniques.

Product	Quantity	Cat. no.
SPoT-Light® CISH™ Hybridizer (120 VAC, 50–60 Hz)	1 each	76-2000
SPoT-Light® CISH™ Hybridizer (240 VAC, 50–60 Hz)	1 each	76-2001
Humidity Control Cards	10 per pack	76-2002

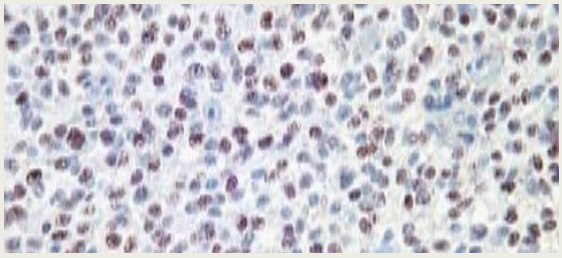

Figure 4—Gene amplification was detected in glioblastoma tissue using a SPoT-Light® EGFR CISH™ probe and CISH™ Polymer Detection Kit (20× magnification).

CISH for a more complete diagnostic picture

"CISH will be very popular with pathologists: you get all the advantages of IHC, including less complex staining protocols, short procedure times, and low-cost permanent slides that can be scored with a routine light microscope, shown to colleagues, and brought to tumor boards."

—Dr. Jeffrey S. Ross, Albany Medical College, Albany, NY

Chromogenic *in situ* hybridization allows detection of gene amplification, gene deletion, chromosome translocations, and chromosome number using conventional peroxidase or alkaline phosphatase reactions under a bright-field microscope on formalin-fixed, paraffin-embedded (FFPE) tissues. Tissue morphology and gene aberrations can thus be viewed simultaneously, and because of its similarities to immunohistochemistry (IHC) techniques, CISH can be easily adapted for use in histology labs. This increases the amount of information available to physicians, helping them make the best therapeutic decisions in patient care.

Invitrogen offers a number of Zymed® SPoT-Light® CISH™ probes and detection kits with potential diagnostic utility in routine histology labs. Probes and detection kits validated for research use include amplification probes (Figure 4), deletion probes, centromeric probes, and translocation probe pairs (Table 2). Learn more at www.invitrogen.com/pathology. ■

References

1. Kosman, D. et al. (2004) *Science* 305:846.
2. Cox, W.G. and Singer, V.L. (2004) *Biotechniques* 36:114–122.

Table 2—SPoT-Light® products for CISH.

Product name	Quantity	Cat. no.	Companion CISH™ Detection Kit	Cat. no.
Amplification probes				
HER2	20 tests	84-0100*†	CISH™ Polymer Kit	84-9246
Cyclin D1	20 tests	84-1900		
EGFr	20 tests	84-1300		
N-Myc	20 tests	84-0400		
Topoll α	20 tests	84-0600		
HER2 CISH Kit	20 tests	84-0146‡	NA	NA
Deletion probes				
19q	20 tests	84-2600	CISH™ Polymer Kit	84-9246
4q12 (PDGFRA)	20 tests	84-3100		
Centromeric probes				
Chromosome 17 Centromeric	20 tests	84-0500	CISH™ Centromere Detection Kit	84-9248
Translocation probe pairs				
BCR/ABL	20 tests	84-1400	CISH™ Bone Marrow/Blood Smear Kit	84-9214
EWS	20 tests	84-0300	CISH™ Translocation Detection Kit	84-9288
SYT	20 tests	84-2500		

Products are for *in vitro* diagnostic use unless otherwise noted.
* Available in the U.S. only. † Analyte specific reagent; analytical and performance characteristics are not established. ‡ Available outside the U.S. only.
NA = not applicable.

Product	Quantity	Cat. no.
FISH Tag™ DNA Green Kit *with Alexa Fluor® 488 dye*	10 rxns	F32947
FISH Tag™ DNA Orange Kit *with Alexa Fluor® 555 dye*	10 rxns	F32948
FISH Tag™ DNA Red Kit *with Alexa Fluor® 594 dye*	10 rxns	F32949
FISH Tag™ DNA Far Red Kit *with Alexa Fluor® 647 dye*	10 rxns	F32950
FISH Tag™ DNA Multicolor Kit *Alexa Fluor® dye combination*	10 rxns	F32951
FISH Tag™ RNA Green Kit *with Alexa Fluor® 488 dye*	10 rxns	F32952
FISH Tag™ RNA Orange Kit *with Alexa Fluor® 555 dye*	10 rxns	F32953
FISH Tag™ RNA Red Kit *with Alexa Fluor® 594 dye*	10 rxns	F32954
FISH Tag™ RNA Far Red Kit *with Alexa Fluor® 647 dye*	10 rxns	F32955
FISH Tag™ RNA Multicolor Kit *Alexa Fluor® dye combination*	10 rxns	F32956

Fluorescent probes for two-photon microscopy

APPLICATIONS IN NEUROSCIENCES AND BEYOND.

Defining characteristics of two-photon excitation

Two-photon excitation (TPE) is a nonlinear optical process first predicted theoretically by Maria Göppert-Mayer in 1931.[1] Its application to fluorescence microscopy was pioneered much more recently by Denk, Strickler, and Webb.[2] In TPE, a fluorophore is excited via near-simultaneous absorption of two photons, each having half the energy (twice the wavelength) required for the transition from the ground to the first singlet excited state (Figure 1). The prerequisite for near-simultaneous absorption and the timescale of molecular light absorption (~10^{-16} seconds) dictates the use of specialized excitation sources; in current instruments, this is typically a mode-locked Ti-Sapphire laser delivering infrared light pulses of femtosecond duration at high repetition rates.[3] Two-photon excited fluorescence has a characteristic dependence on the square of the excitation light intensity—doubling the excitation intensity quadruples the fluorescence signal. In contrast, fluorescence derived from conventional one-photon absorption exhibits linear dependence on excitation light intensity.

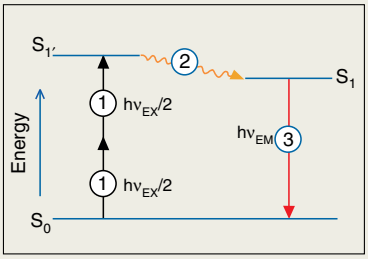

Figure 1—Excited state energy diagram showing two-photon excitation (1) followed by nonradiative vibrational relaxation (2) and spontaneous fluorescence photon emission (3). In conventional fluorescence detection systems, excitation is achieved by absorption of a single photon of energy hu_{EX}; processes (2) and (3) are essentially the same.

There are many practical benefits to using TPE, given the transparency of tissues to infrared excitation light:

- spatial confinement of fluorescence to a very small volume (~0.1 µm^3) defined by the focused excitation light, providing inherent 3D imaging capability (Figure 2)
- capacity for imaging at increased depths in tissues[4]
- confinement of photodamage and photobleaching effects to the excitation volume, resulting in increased viability of living specimens[5,6]

Figure 2—An experiment illustrating ordinary (single-photon) excitation of fluorescence and two-photon excitation. The cuvette contains a solution of the dye safranin O, which normally emits yellow light when excited by green light. The upper lens focuses green (543 nm) light from a CW helium–neon laser into the cuvette, producing the expected conical pattern of excitation (fading to the left). The lower lens focuses pulsed infrared (1,046 nm) light from a neodymium–YLF laser. In two-photon absorption, the excitation is proportional to the square of the intensity; thus, the emission is confined to a small point focus (see arrow), which can be positioned anywhere in the cuvette by moving the illuminating beam. Image contributed by Brad Amos, Science Photo Library, London.

However, in addition to requiring specialized (and therefore fairly expensive) excitation sources, TPE produces photodamage and photobleaching effects within the confined excitation volume that are often more acute than those produced by laser scanning confocal microscopy.[7–10] The advantages of TPE primarily relate to imaging of living specimens. Accordingly, neuroscience—specifically structural and functional imaging of the nervous system—is the largest field of current applications (Table 1). In addition to providing benefits for fluorescence microscopy, TPE offers advantages in other biophotonic techniques such as fluorescence correlation spectroscopy,[11] controlled photoablation,[12] photodynamic therapy,[13] and activation of "caged" compounds.[14] To learn more about the technical foundations and applications of TPE microscopy, researchers should consult the growing collection of available review literature.[15–20]

Table 1—Selected applications of fluorescent probes for two-photon excitation (TPE) microscopy.

Probe	Cat. no.	TPE excitation wavelength	Application	References
Alexa Fluor® 488 phalloidin	A12379	720 nm or 830 nm	Imaging F-actin organization in pancreatic acinar cells	*J Biol Chem* 279:37544–37550 (2004)
Alexa Fluor® 594 hydrazide	A10438, A10442	810 nm	Ca^{2+}-insensitive, neuronal tracer *	*Neuron* 33: 439–452 (2002); www.stke.org/cgi/content/full/sigtrans;2004/219/pl5
Amplex® Red reagent	A12222, A22177	750 nm or 800 nm	Detection of reactive oxygen species (ROS) associated with amyloid plaques	*J Neurosci* 23:2212–2217 (2003)
CFSE, CMTMR	C1157, C2927	820 nm	Tracking T- and B-lymphocyte and dendritic cell motility patterns in intact mouse lymph nodes †	*Science* 296: 1869–1873 (2002); *Proc Natl Acad Sci U S A* 101: 998–1003 (2004)
CM-H_2DCFDA	C6827	740 nm	Detection of localized reactive oxygen species release in cardiomyocytes ‡	*J Biol Chem* 278: 44735–44744 (2003)
DAPI, Hoechst 33342	D1306, D3571, D21490, H1399, H3570, H21492	740 nm	Imaging DNA in nuclei and isolated chromosomes	*Micron* 32:679–684 (2001); *Histochem Cell Biol* 114:337–345 (2000)
DiD	D307, D7757	817 nm	Intravital imaging of mouse erythrocytes	*Proc Natl Acad Sci U S A* 102:16807–16812 (2005)
FM® 1-43	T3163, T35356	840 nm	Monitoring synaptic vesicle recycling in rat brain slices	*Biotechniques* 40:343–349 (2006)
Fluo-5F §	F14221, F14222	810 nm	Imaging Ca^{2+} concentration dynamics in dendrites and dendritic spines	*Neuron* 33:439–452 (2002); www.stke.org/cgi/content/full/sigtrans;2004/219/pl5
Fura-2	F1200, F1201, F1221, F1225, F6799, F14185	780 nm	Detection of GABA-mediated Ca^{2+} transients in rat cerebellar Purkinje neurons	*J Physiol* 536:429–437 (2001)
Lucifer yellow CH	L453, L682, L1177	850 nm	Identification of gap junctions in rat brain slices	*J Neurosci* 23:9254–9262 (2003)
Laurdan	D250	800 nm	Detection of ordered membrane lipid domains	*Proc Natl Acad Sci U S A* 100:15554–15559 (2003); *J Cell Biol* 174:725–734 (2006)
Monochlorobimane	M1381MP	780 nm	Imaging glutathione levels in rat brain slices and intact mouse brain	*J Biol Chem* 281:17420–17431 (2006)
MQAE	E3101	750 nm	Fluorescence lifetime imaging (FLIM) of intracellular Cl^- concentrations in olfactory sensory neurons	*J Neurosci* 24:7931–7938 (2004)
Oregon Green® 488 BAPTA-1	O6806, O6807	880 nm	Imaging spatiotemporal relationships of Ca^{2+} signals among cell populations in rat brain cortex	*Proc Natl Acad Sci U S A* 102:14063–14068 (2005)
Qdot® 525, Qdot® 585, Qdot® 655 nanocrystals	Q11441MP, Q10111MP, Q11621MP, Q11421MP	750 nm	Multiplexed immunohistochemical analysis of arterial walls **	*Am J Physiol* 290:R114–R123 (2006)
SBFI	S1262, S1263, S1264	760 nm	Imaging of intracellular Na^+ gradients in rat cardiomyocytes	*Biophys J* 87:1360–1368 (2004)
TMRE	T669	740 nm	Mitochondrial membrane potential sensor ‡	*J Biol Chem* 278:44735–44744 (2003)
X-rhod-1	X14209, X14210	900 nm	Simultaneous imaging of GFP-PHD translocation and Ca^{2+} dynamics in cerebellar purkinje cells	*J Neurosci* 24:9513–9520 (2004)

* Used in combination with fluo-4, fluo-5F, or fluo-4FF to obtain ratio signals that are insensitive to small changes in resting Ca^{2+} and are independent of subcellular compartment volume. † Multiplexed (single excitation/dual channel emission) combination of CFSE and CMTMR. § Techniques also applicable to fluo-4 and fluo-4FF indicators. ‡ Multiplexed (single excitation/dual channel emission) combination of TMRE and CM-H_2DCFDA. ** Multiplexed (single excitation/dual channel emission) combination of Qdot® 585 and Qdot® 655 nanocrystals. PHD = pleckstrin homology domain.

Fluorescence excitation and emission spectra

One-photon and two-photon excitation of a given fluorophore generally result in identical fluorescence emission spectra, as the originating excited state and the photon emission process are the same (Figure 1). However, two-photon excitation spectra differ from their one-photon counterparts to an extent that depends on the molecular orbital symmetry of the fluorophore (greater difference for higher symmetry fluorophores).[18] Consequently, most two-photon excitation spectra are blue-shifted and broader compared to the corresponding one-photon spectra plotted on a doubled wavelength axis. Simply stated, a fluorophore with a one-photon excitation peak at 500 nm will probably have a two-photon excitation maximum at <1,000 nm (Figure 3). Because two-photon excitation spectra are relatively broad, multiplex detection schemes in which two or more fluorophores are excited at a single wavelength and discriminated on the basis of different emission spectra are relatively easy to implement (some examples are included in Table 1). The two-photon absorption cross-section (σ) in units of GM (for Göppert-Mayer; 1 GM = 10^{-50} cm^4 seconds) quantifies the efficiency of TPE for different fluorophores and is plotted on the y-axis of excitation spectra (Figure 3). There are several published collections of two-photon excitation spectra and cross-sections that provide guidance on compatibility of dyes and probes with excitation sources.[21–25] Excitation wavelengths used in selected published TPE microscopy applications are listed in Table 1.

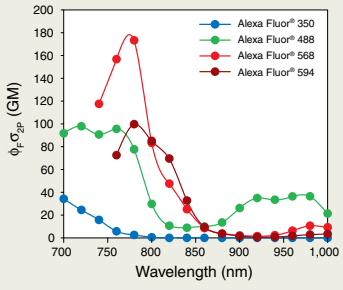

Figure 3—Two-photon excitation spectra of Alexa Fluor® 350, Alexa Fluor® 488, Alexa Fluor® 568, and Alexa Fluor® 594 dyes. The y-axis units are products of fluorescence quantum yields (Φ_F) and two-photon absorption cross-sections (σ). Data courtesy of Warren Zipfel, Cornell University.

Fluorophores and probes

TPE has added a new spectral dimension to fluorescence microscopy. Probes such as fura-2 (Ca^{2+}), SBFI (Na^+), monochlorobimane (glutathione), and DAPI (nuclear DNA), which were previously of limited utility in confocal microscopy due to their requirements for ultraviolet excitation, now have a new lease on life (Table 1). Furthermore, *in situ* imaging of small endogenous fluorophores such as serotonin and NADH that are almost inaccessible to one-photon excitation has now become practicable.[26] Organic fluorophores and fluorescent proteins typically have two-photon absorption cross-sections in the range 1–100 GM. However, fluorophores with smaller cross-sections (e.g., NADH, σ < 0.1 GM) can still generate sufficient TPE fluorescence for imaging purposes.[26] At the opposite extreme, Qdot® nanocrystals have cross-sections exceeding 10,000 GM, promising even further expansions to the utility of TPE imaging, particularly in the area of *in vivo* applications.[27,28] ■

References

1. Göppert-Mayer, M. (1931) *Ann Phys* 9:273–294.
2. Denk, W. et al. (1990) *Science* 248:73–76.
3. Girkin, J.M. and McConnell, G. (2005) *Micros Res Tech* 67:8–14.
4. Helmchen, F. and Denk, W. (2005) *Nat Methods* 2:932–940.
5. Squirrell, J.M. et al. (1999) *Nature Biotech* 17: 763–767.
6. Ruthazer, E.S. and Cline, H.T. (2002) *Real-Time Imaging* 8:175–188.
7. Eggeling, C. et al. (2005) *Chemphyschem* 6:791–804.
8. Hopt, A. and Neher, E. (2001) *Biophys J* 80:2029–2036.
9. Patterson, G. H. and Piston, D.W. (2000) *Biophys J* 78:2159–2162.
10. Dittrich, P.S. and Schwille, P. (2001) *Appl Phys B* 73:829–837.
11. Larson, D.R. et al. (2005) *J Cell Biol* 171:527–536.
12. Galbraith, J.A. and Terasaki, M. (2003) *Mol Biol Cell* 14:1808–1817.
13. Karotki, A. et al. (2006) *Photochem Photobiol* 82:443–452.
14. Brown, E.B. and Webb, W.W. (1998) *Methods Enzymol* 291:356–380.
15. Svoboda, K. and Yasuda, R. (2006) *Neuron* 50:823–839.
16. Diaspro, A. et al. (2005) *Q Rev Biophys* 38:97–166.
17. Rubart, M. (2004) *Circ Res* 95:1154–1166.
18. Zipfel, W.R. et al. (2003) *Nature Biotech* 21:1369–1377.
19. Helmchen, F. and Denk, W. (2005) *Nat Methods* 2:932–940.
20. Denk, W. et al. (2006) *Handbook of Biological Confocal Microscopy, Third Edition* (Pawley, J.B., Ed.), Springer, pp. 535–549.
21. Xu, C. et al. (1996) *Proc Natl Acad Sci U S A* 93:10763–10768.
22. Bestvater, F. et al. (2002) *J Microscopy* 208: 108–115.
23. Dickinson, M.E. et al. (2003) *J Biomed Opt* 8: 329–338.
24. Fisher, J.A. et al. (2005) *J Neurosci Methods* 148: 94–102.
25. Wokosin, D.L. et al. (2004) *Biophys J* 86:1726–1738.
26. Zipfel, W.R. et al. (2003) *Proc Natl Acad Sci U S A* 100:7075–7080.
27. Larson, D.R. et al. (2003) *Science* 300:1434–1436.
28. Michalet, X. et al. (2005) *Science* 307:538–544.

New applications for Vybrant® DyeCycle™ stains

IDENTIFYING STEM CELL SIDE POPULATIONS AND CELL CYCLE–BASED SORTING.

Live-cell studies of cellular DNA content and cell cycle distribution are useful to detect variations of growth patterns due to a variety of physical, chemical, or biological means, to monitor apoptosis, and to study tumor behavior and suppressor gene mechanisms. The Vybrant® DyeCycle™ stains, available as Vybrant® DyeCycle™ Violet stain, Vybrant® DyeCycle™ Green stain, and Vybrant® DyeCycle™ Orange stain, were designed to report DNA content in living cells. All Vybrant® DyeCycle™ stains are DNA selective, cell membrane permeant, and nonfluorescent until bound to double-stranded DNA. These dyes take advantage of the commonly available 488 nm and violet excitation sources, placing cell cycle studies within reach of all flow cytometrists.

Recent studies have shown the utility of these dyes in two new application areas:

- identification of stem cell side populations (SP) [1] (Figure 1)
- sorting potential based on cell cycle phase (Figure 2)

Identification of Hoechst side population using DyeCycle™ Violet stain

Hoechst 33342 is widely used as a reagent to identify stem cells and early progenitors in mammalian hematopoietic tissues. After loading a cell population with Hoechst 33342, a cell-permeant nucleic acid stain, the side population (SP) containing stem cells and early progenitors is identified in the cytometer as a low-fluorescence "tail" (arising as the dye is pumped out of the cell via an ABCG2 membrane pump–dependent mechanism). This technique requires a flow cytometer equipped with a UV laser, an uncommon and relatively costly option. As violet diode lasers become more prevalent secondary excitation sources on flow cytometers, the opportunity arises for performing this technique using a violet laser–excited cell-permeant nucleic acid stain. DyeCycle™ Violet stain exhibits the same pump specificity as Hoechst 33342 while being excited by the violet laser.

With DyeCycle™ Violet stain in mouse hematopoietic cells, side populations similar to those observed with Hoechst 33342 can be resolved using either violet or UV excitation (Figure 1). Fumitremorgin C, an ABCG2-specific inhibitor, blocked the appearance of this cell population. Further characterization of the cells by immunophenotyping using mouse bone marrow stem cell markers confirmed that the identified DyeCycle™ Violet stain SP is restricted to the stem cell LSK population (Lineage^{negative} Sca-1^{positive} c-kit^{positive}), similar to the Hoechst 33342 SP. These results strongly suggest that DyeCycle™ Violet stain efflux identified the same stem cell population as Hoechst 33342 efflux.* SP analysis on flow cytometers equipped with violet lasers should therefore be possible by substituting DyeCycle™ Violet stain for Hoechst 33342.

* For details of this experiment, visit **www.invitrogen.com/flowcytometry** and follow the link under the poster entitled "Cell Cycle Analysis in Live Cells Using Novel Vybrant® DyeCycle™ Stains."

Cell sorting using Vybrant® DyeCycle™ stains

Flow cytometry testing is useful for quantifying the distribution of cell populations across the different nuclear phases of the cell cycle. Analysis of the cell cycle is widely used in cell growth and cell cycle regulation studies, oncology research, and DNA ploidy determinations. These applications require dyes that bind to DNA in a stoichiometric manner. With the exceptions of UV-excited dyes such as Hoechst 33342, cells have generally required fixation and permeabilization as well as treatment with RNase to obtain DNA-specific cell cycle information. The Vybrant® DyeCycle™ stains are DNA-selective, cell membrane–permeant dyes that show greatly enhanced fluorescence when bound to DNA and are available in versions that can be excited by 405 nm, 488 nm, or 532 nm lasers. Cell cycle analysis using the Vybrant® DyeCycle™ stains has been performed on a wide variety of cells, including Jurkat, CHO, 3T3, and HL60 cells, and peripheral blood lymphocytes, monocytes, and neutrophils.

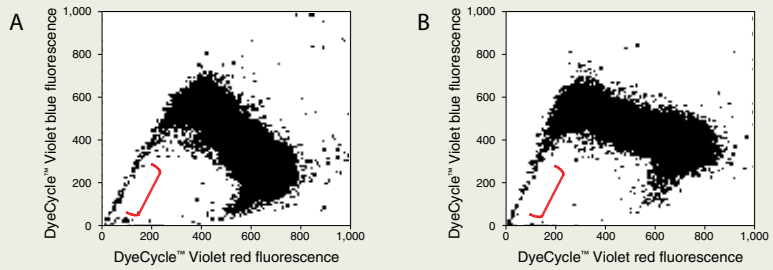

Figure 1—DyeCycle™ Violet stain side population analysis in human cord blood. Cells were incubated with 10 µM DyeCycle™ Violet stain for 90 minutes at 37°C, then washed and stored on ice until analysis. Results were the same using UV excitation (A) or violet diode laser excitation (B). Data courtesy of William Telford, NIH.

Because DyeCycle™ dyes can be used for cell cycle analysis on living cells, experiments were performed to determine whether these dyes could be used to sort cell populations based on their position within the cell cycle. HEK and NIH3T3 cells were stained with DyeCycle™ Violet and DyeCycle™ Orange stains, respectively, then sorted using a BD FACSVantage™ flow cytometer. Figure 2 shows NIH3T3 cells stained with DyeCycle™ Orange stain. While the Vybrant® DyeCycle™ stains caused some retardation of cell division, they did not produce the toxicity reported with DRAQ5™ stain (Biostatus Ltd.) and have been used to sort viable cells from G_0/G_1 and G_2/M populations. Resolution of cell cycle information in viable cells allows evaluation against the dynamic background of live-cell activity, as well as the possibility of cell sorting based on position in the cell cycle. ■

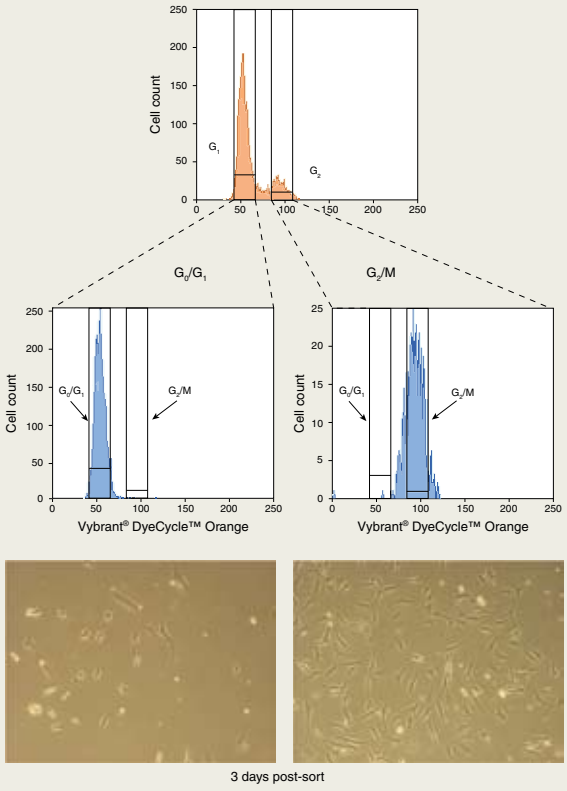

Figure 2—Sorting of live-cell populations. NIH3T3 cells were stained with 10 µM Vybrant® DyeCycle™ Orange stain. Cells were sorted based on G_0/G_1 and G_2/M gates using a FACSVantage™ flow cytometer (BD Biosciences) with 488 nm excitation and a 585/42 nm bandpass filter. Cells were cultured after sorting.

Reference

1. Telford, William G. et al. (2007) *Stem Cells* (in press).

Product	Excitation	Quantity	Cat. no.
Vybrant® DyeCycle™ Violet stain *5 mM in water* *200 assays*	UV, 405 nm	200 µl	V35003
Vybrant® DyeCycle™ Green stain *5 mM solution in DMSO* *200 assays*	488 nm	400 µl	V35004
Vybrant® DyeCycle™ Orange stain *5 mM solution in DMSO* *200 assays*	488 nm, 532 nm	400 µl	V35005

JOURNAL HIGHLIGHT

A new approach to cell-based multiplexing expands the drug screening capabilities of flow cytometry

Krutzik, P.O. and Nolan, G.P. (2006) Fluorescent Cell Barcoding in Flow Cytometry Allows High-Throughput Drug Screening and Signaling Profiling. *Nature Methods* 5:361–368.

Can high-throughput, high-content flow cytometry be economically applied to large-scale drug screening? Flow cytometry is a widely utilized and powerful method for the analysis of multiple antigens in cell populations. However, the use of flow cytometry in drug screening applications, which can involve hundreds or thousands of samples, can quickly become cost and time prohibitive, due to the amounts of antibodies required and the throughput limitations of cytometers. The authors present a cell-based multiplexing approach—fluorescent cell barcoding (FCB)—that uses varied staining intensities to allow the analysis of complex samples in a single flow cytometry run.

In this technique (based on standard phospho flow protocols), cell samples that have undergone an initial treatment (e.g., unstimulated, stimulated, and stimulated in the presence of an inhibitor drug candidate) are "barcoded" by general staining with different levels of a reactive fluorophore (Pacific Blue™, Alexa Fluor® 488, Alexa Fluor® 700, and Alexa Fluor® 750 fluorophores were all shown to be effective barcoding dyes). Following barcoding, the samples are then recombined, stained with fluorescently labeled antibodies to detect the effects of the treatment, and analyzed as a single sample. Deconvolution of the results clearly resolves the differentially treated cells into discrete, quantifiable populations. The authors successfully demonstrate the utility of the method for real-world drug screening applications. In an inhibitor-titration experiment using the Pacific Blue™ fluorophore as the barcoding dye, U937 monocyte cells were pretreated with four small-molecule inhibitors of JAK kinases, then stimulated to induce pStat1, pStat3, and pStat5 production. The effect of these inhibitors on the degree of phosphorylation of the three Stat transcription factors was clearly revealed in a single flow cytometry run.

In a separate experiment—a 96-well plate–based drug candidate screening application—the authors employed a three-dye FCB barcoding scheme to label 96 samples. They used this scheme to screen a library of 70 small-molecule inhibitors for their effect on T cell receptor–mediated ERK phosphorylation/Stat1 phosphorylation in response to interferon-γ (IFN-γ) treatment. This screening experiment was completed in a single 5 minute flow cytometry run, and identified two compounds that selectively inhibited one or the other pathway and three compounds that nonselectively affected both pathways.

Overall, the authors report up to 100-fold reduction in antibody consumption, with significantly less acquisition time required for complex sample analyses. Owing to its improved throughput and greatly reduced consumption of antibodies, the FCB methodology may prove useful for drug candidate screening as well as for clinical monitoring of patient samples during late-stage drug trials.

Product	Quantity	Cat. no.
Alexa Fluor® 488 carboxylic acid, succinimidyl ester *mixed isomers*	1 mg	A20000
Alexa Fluor® 488 carboxylic acid, succinimidyl ester *mixed isomers*	5 mg	A20100
Alexa Fluor® 700 carboxylic acid, succinimidyl ester *mixed isomers*	1 mg	A20010
Alexa Fluor® 700 carboxylic acid, succinimidyl ester *mixed isomers*	5 mg	A20110
Alexa Fluor® 750 carboxylic acid, succinimidyl ester *mixed isomers*	1 mg	A20011
Alexa Fluor® 750 carboxylic acid, succinimidyl ester *mixed isomers*	5 mg	A20111
Pacific Blue™ succinimidyl ester	5 mg	P10163

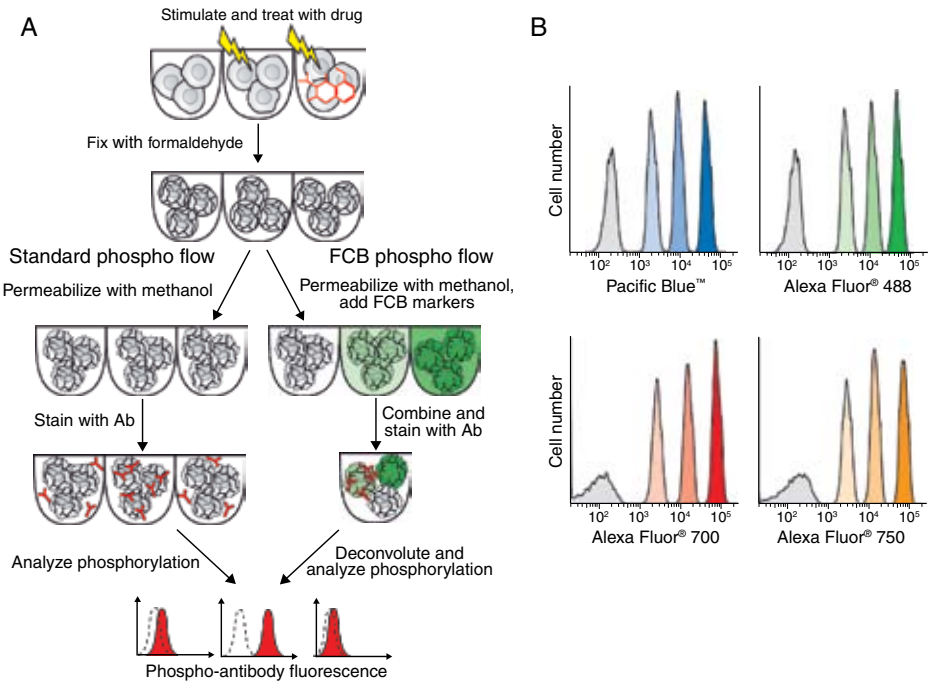

Figure 1—The fluorescent cell barcoding (FCB) technique. (A) Sample one was unstimulated, sample two was stimulated, and sample three was treated with a small-molecule inhibitor before stimulation. After fixation, cells in standard phospho flow (left) were permeabilized with cold methanol, washed, and stained with phospho-specific antibodies. In the FCS technique (right side), each sample was permeabilized with 20–25°C methanol containing a different concentration of amine-reactive fluorescent dyes (FCB markers), yielding a unique fluorescence signature for each sample. Samples were then washed, combined into one tube, and stained with antibodies. During software analysis of the acquired data, the samples were deconvoluted back to the original samples based on their FCB signature. In both standard and FCB phospho flow techniques, fluorescence of the phospho-specific antibody in each sample was measured. In the plots, dotted lines indicate autofluorescence and red histograms represent sample fluorescence. (B) Efficient labeling of four samples per marker with the FCB technique. U937 cells were fixed, then permeabilized in methanol containing 0, 0.04, 0.2, or 1 µg/ml Pacific Blue™–NHS, Alexa Fluor® 488–NHS, Alexa Fluor® 700–NHS, or 0, 0.4, 2, or 10 µg/ml Alexa Fluor® 750–NHS for 15 minutes at 20–25°C. After washing twice, samples stained with each FCB marker were combined and analyzed. Shown are histograms identifying the four original samples barcoded with each FCB marker. Gray peaks represent unlabeled samples (zero FCB marker). Colored peaks represent samples receiving low, medium, and high amounts of the FCB marker, with color intensity correlating to FCB marker staining level. Image reproduced from *Nature Methods* 3:361–368 (2005); used with permission.

Dead-cell discrimination in a different light

SYTOX® RED DEAD CELL STAIN.

Thousands of flow cytometry runs every day rely on dead-cell discrimination either as an endpoint result or as one parameter in a broader experimental query. Fluorescent markers for dead-cell staining are therefore indispensable reagents for flow cytometric analysis.

Propidium iodide (PI) has widely been utilized as a stain to differentiate live and dead cells in flow cytometry experiments. Because of its broad emission spectrum, multiple detection channels on the flow cytometer are occupied when PI is used, which limits the number of parameters that can be detected in a given experiment. In addition, the emission of PI directly overlaps the emission of R-phycoerythrin (R-PE), making PI incompatible with R-PE–labeled probes. Dead-cell stains that can be excited by light sources other than the 488 nm laser are highly sought-after reagents because they allow the 488 nm laser to be reserved for bright fluorochromes on antibodies directed against challenging antigens.

SYTOX® Red dead cell stain is a high-affinity nucleic acid stain that easily penetrates cells with compromised plasma membranes, but will not cross intact cell membranes. After a brief incubation with SYTOX® Red stain (excitation/emission ~640/658 nm), the nucleic acids of dead cells fluoresce bright red when excited with 633 or 635 nm laser light. And because SYTOX® Red dead cell stain does not rely on the 488 nm laser and has an emission signal limited to one channel, adding it to other dyes in multicolor flow cytometry experiments is easy. For example, staining an ammonium chloride–lysed whole blood sample with mouse anti–human CD4 R-PE Alexa Fluor® 700, mouse anti–human CD8 R-PE, and mouse anti–human CD3 Alexa Fluor® 488 for 30 minutes, followed by 5 µM SYTOX® Red stain, allowed easy gating on the live-cell population and clear visualization of the various immunophenotypes (Figure 1). These properties, combined with its >500-fold fluorescence enhancement upon nucleic acid binding, make the SYTOX® Red dead cell stain a simple and quantitative single-step dead-cell indicator for use with red laser–equipped flow cytometers. ■

Product	Quantity	Cat. no.
SYTOX® Red dead cell stain *for 633 or 635 nm excitation* *5 µM solution in DMSO*	1 ml	S34859

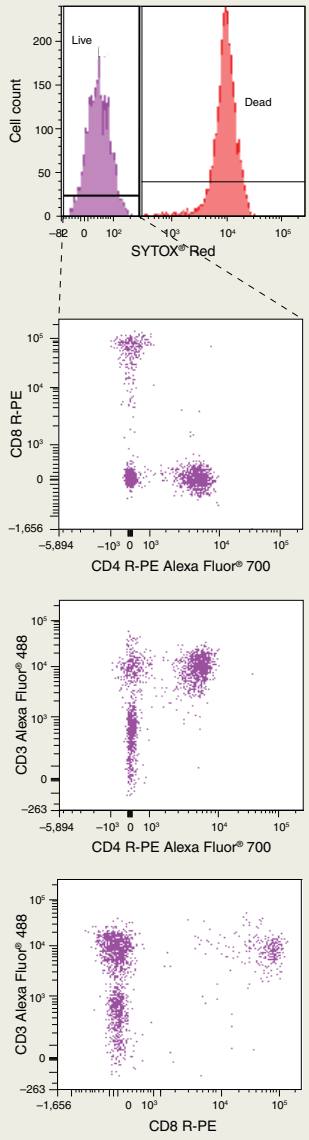

Figure 1—Illuminate your samples with better dead-cell discrimination. The blood cell sample was stained as described in the text. Using a BD™ LSR II system (BD Biosciences), the sample was gated on lymphocytes and on cells negative for SYTOX® Red stain. Fluorescence was monitored using 488 and 633 nm excitation and 530/30, 585/42, 720/20, and 660/20 nm bandpass filters.

PRODUCT HIGHLIGHT

Streptavidin conjugates of R-phycoerythrin—detection workhorses

R-phycoerythrin (R-PE), a fluorescent protein derived from eukaryotic algae, contains covalently linked tetrapyrrole groups that collect light and, through fluorescence resonance energy transfer (FRET), convey it to a pair of chlorophyll molecules located in the photosynthetic reaction center.[1] Because of its role in light collection, R-PE has evolved to maximize both absorption and fluorescence emission and to minimize the quenching caused either by internal energy transfer or by external factors such as changes in pH or ionic composition.[2] R-PE has several advantages over organically synthesized fluorophores such as fluorescein, including a very high extinction coefficient (1,960,000 $cm^{-1}M^{-1}$) and an excellent quantum yield. The result is a molecule with fluorescence equivalent to at least 30 unquenched fluorescein or 100 rhodamine molecules at comparable wavelengths.

Streptavidin conjugates of R-PE have become the trusted workhorses of flow cytometry, microarray, and Luminex® technology–based applications. While conjugation of R-PE to streptavidin does reduce the molecule's fluorescence somewhat, in practical applications the sensitivity of an R-PE conjugate is typically 5–10 times that of the corresponding fluorescein conjugate.[3] As an added advantage, streptavidin R-PE conjugates can be efficiently excited and detected using a number of standard excitation source and emission filter combinations (see figure below).

Molecular Probes was the first company to offer R-PE–conjugated products, and as part of Invitrogen we have continued to optimize the production process. Molecular Probes® streptavidin R-PE conjugates are purified by HPLC to remove most aggregates and free R-phycoerythrin, minimizing background and improving the overall signal-to-noise ratio. Our HPLC methods also allow us to achieve high levels of lot-to-lot consistency, which means highly reproducible results for your experiments. Our streptavidin R-PE conjugates also come highly recommended—Affymetrix recommends Molecular Probes® streptavidin R-PE for their GeneChip® protocols.

Molecular Probes® streptavidin R-PE conjugates are available from Invitrogen in standard (S866) and premium (S21388) grades. The standard grade product is suitable for most flow cytometry and microarray applications; the premium grade product represents a further fractionation of the conjugates and is designed for applications that require extremely low background levels, such as the detection of very low abundance targets. For additional technical details, including spectra, please see Section 6.4 of *The Handbook* at **probes.invitrogen.com/handbook**.

References

1. MacColl. R.J. (1991) *J Fluoresc* 1:135–140.
2. Glazer, A.N. (1989) *J Biol Chem* 264:1–4.
3. Kronick, M.N. and Grossman, P.D. (1983) *Clin Chem* 29:1582–1586.

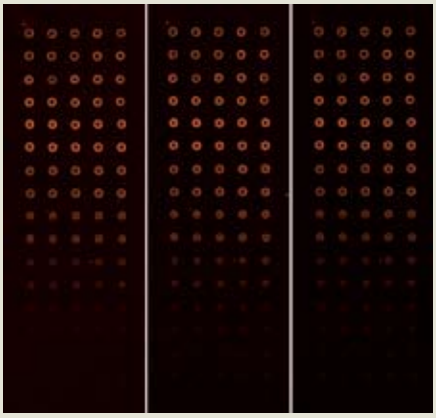

Streptavidin R-PE used to detect biotinylated DNA on a microarray. The fluorescence signal was detected using three different detection configurations: 488 nm excitation (argon-ion laser)/570 nm emission filter (left); 543.5 nm excitation (He–Ne laser)/570 nm emission filter (center); 543 nm excitation (He–Ne laser)/592 nm emission filter (right).

Product	Quantity	Cat. no.
streptavidin, R-phycoerythrin conjugate (SAPE) *1 mg/ml*	1 ml	S866
streptavidin, R-phycoerythrin conjugate (SAPE) *premium grade* *1 mg/ml*	1 ml	S21388

Highly sensitive methods for phosphate detection

THREE ASSAY FORMATS ALLOW YOU TO MEASURE PHOSPHATE LEVELS WHEN—AND HOW—YOU WANT.

Numerous enzymes of therapeutic relevance produce inorganic phosphate directly, or through coupled reactions. These potential drug targets include lipid and protein phosphatases, ATPases, GTPases, prenyltransferases, and phosphodiesterases. The very nature of these targets makes high-quality phosphate assays indispensable to drug discovery research. Here we discuss three assay formats (Table 1) designed to meet different phosphate measurement sensitivity needs depending on sample size and type.

For sensitive, miniaturizable measurements

To address the need for sensitive and miniaturizable phosphate detection, Invitrogen offers Phosphate Sensor. Phosphate Sensor is a purified form of recombinant *E. coli* phosphate-binding protein labeled with the fluorophore MDCC, which is sensitive to changes in its environment (Figure 1). Phosphate binding is tight (K_d ~100 nM), enabling detection in the submicromolar range, which is orders of magnitude more sensitive than the commonly used malachite green (Figure 2). Furthermore, because binding of phosphate is rapid, Phosphate Sensor can be used to monitor phosphate formation in real time, unlike malachite green.

For quantitative, versatile measurements

The P_iPer™ Phosphate Assay Kit also detects in the submicromolar range. Based upon the Amplex® Red reagent, the P_iPer™ Kit enables detection by fluorescence or absorbance. This enzyme-coupled assay ultimately relies on the robust 1:1 stoichiometric reaction between the Amplex® Red reagent and H_2O_2 in the presence of horseradish peroxidase (HRP). The nonfluorescent Amplex® Red reagent produces resorufin, a brightly fluorescing, strongly absorbing reaction product that possesses good quantum efficiency and a high extinction coefficient for a truly quantitative measurement of phosphate. Additionally, because of the long-wavelength spectra, there is little interference from the blue or green autofluorescence found in most biological samples.

Table 1—Spectral properties for Invitrogen™ phosphate assays.

Assay	Abs/Ex*	Em†
Phosphate Sensor	419	466
P_iPer™ Phosphate Assay Kit	563	587
EnzChek® Phosphate Assay Kit	360	NA

* Absorbance or fluorescence excitation maxima, in nm. † Emission maxima, in nm. NA = not applicable.

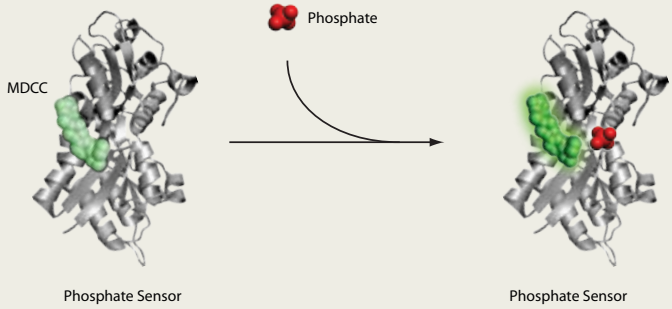

Figure 1—The mechanism behind the Phosphate Sensor reagent. Phosphate Sensor contains a single MDCC fluorophore near the phosphate-binding site. Upon binding phosphate, the fluorescence intensity of the bright blue fluorophore increases dramatically.

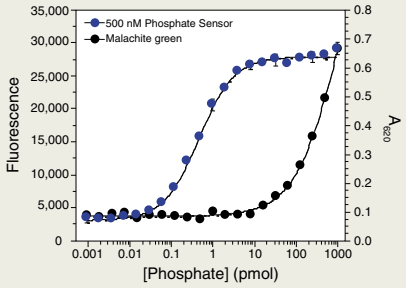

Figure 2—The sensitivity of Phosphate Sensor compared to a malachite green–based reagent. Phosphate standards (10 µl) were added to 384-well plates (clear bottom for malachite green). Either malachite green reagent (70 µl) or Phosphate Sensor (10 µl of 1 µM stock) was added to each well. Absorbance at 620 nm was measured for malachite green. Fluorescence measurements were captured for Phosphate Sensor using a Tecan Safire2™ plate reader with excitation at 430 nm (10 nm bandwidth) and emission at 450 nm (10 nm bandwidth).

For use with more concentrated samples

The absorbance-based EnzChek® Phosphate Assay Kit has an assay range of 2–150 µM, eliminating the need to dilute samples of higher concentration. This assay uses the spectrophotometric shift from 330 nm to 360 nm caused by the phosphorylation of the substrate MESG in the presence of purine nucleoside phosphorylase (PNP) to indicate phosphate levels.

For complete information on Invitrogen's phosphate detection assay portfolio, visit **www.invitrogen.com/phosphate**. ■

PRODUCT HIGHLIGHT

Amplex® Red/UltraRed stop reagent

Stop horseradish peroxidase (HRP) reactions in their tracks. This stop reagent offers unparalleled convenience and control, in addition to:

- compatibility with all Amplex® Red assays and Amplex® Red/UltraRed stand-alone reagents
- a stable fluorescent signal for at least 3 hours
- the ability to terminate reactions containing up to 0.1 units/ml HRP and 5 µM H_2O_2

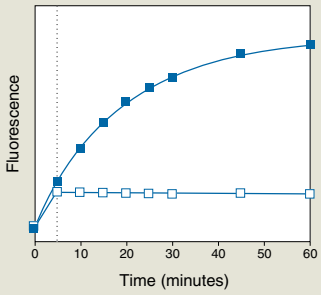

Application of the Amplex® Red/UltraRed stop reagent to control H_2O_2/peroxidase–coupled detection reactions. Two parallel reactions containing 0.5 mU/ml horseradish peroxidase (HRP) in 50 mM sodium phosphate buffer, pH 7.4, were initiated by addition of 50 µM Amplex® Red reagent + 1 mM H_2O_2. Reaction progress was monitored by detection of the fluorescent product resorufin at 37°C in a fluorescence microplate reader using excitation at 530 ± 12.5 nm and fluorescence detection at 590 ± 17.5 nm. After five minutes (⁘), one of the reactions (□) was terminated by addition of Amplex® Red/UltraRed stop reagent. The fluorescence signal in the stopped reaction remained at the constant level shown for 3 hours (data not shown).

Product	Quantity	Cat. no.
Amplex® Red/UltraRed stop reagent *500 tests* *set of 5 vials*	1 set	A33855

Product	Quantity	Cat. no.
Phosphate Sensor	10 nmol (1,000 assays)	PV4406
Phosphate Sensor	100 nmol (10,000 assays)	PV4407
P_iPer™ Phosphate Assay Kit	1,000 assays	P22061
EnzChek® Phosphate Assay Kit	100 assays	E6646

Omnia™ Kinase Assays

MEASURE KINASE ACTIVITY IN REAL TIME.

Protein kinases are an important class of enzymes that contribute substantially to overall proteomic diversity and signal transduction in normal and disease states. As a result, this group of 518 serine/threonine (Ser/Thr) and tyrosine (Tyr) kinases is being actively pursued as drug targets for disease intervention. Now you can gain more information from your studies with the Omnia™ Kinase Assays. These easy-to-use, fluorescence-based protein kinase assays provide a rapid, homogeneous, and sensitive method for detecting enzymatic activity. Omnia™ Assays provide real-time results under optimal kinetic conditions, with minimal interference from exogenous phosphate or autofluorescence.

Advantages of the Omnia™ platform

The Omnia™ platform measures kinase activity in real time using the Sox fluorophore, which was developed by Barbara Imperiali.[1–4] Importantly, it directly and selectively measures the amount of phosphate that is transferred to a peptide substrate during the reaction without the need for antibodies, beads, radioactive ATP, or secondary detection steps, as is typically required with other assays. Results are obtained instantaneously, allowing you to monitor the kinase reaction continuously in kinetic mode. With real-time kinetics, measurements are based on reaction rates, which contributes to the very high precision of the Omnia™ Assays and corrects for any compound autofluorescence. In addition, the Omnia™ Kinase Assay platform can be used in a variety of cell-based assay formats, including plate and bead immunoprecipitation-based kinase assays and direct analysis of crude cell lysates, and is compatible with 96-, 384-, and 1536-well plates.

The basis of detection

The Omnia™ Kinase Assays use peptide substrates that contain a chelation-enhanced fluorophore, 8-hydroxy-5-(*N*, *N*-dimethylsulfonamido)-2-methylquinoline (referred to as Sox), to create real-time biosensors that provide a direct fluorescence-based measure of kinase activity.[1–4] Upon phosphorylation, Mg^{2+} is chelated between the newly added phosphate group and the Sox moiety, forming a complex that causes an increase in fluorescence from the Sox residue (Figure 1). Importantly, this type of complex can only be formed between the Sox moiety and the phosphate group on the side chain of the targeted

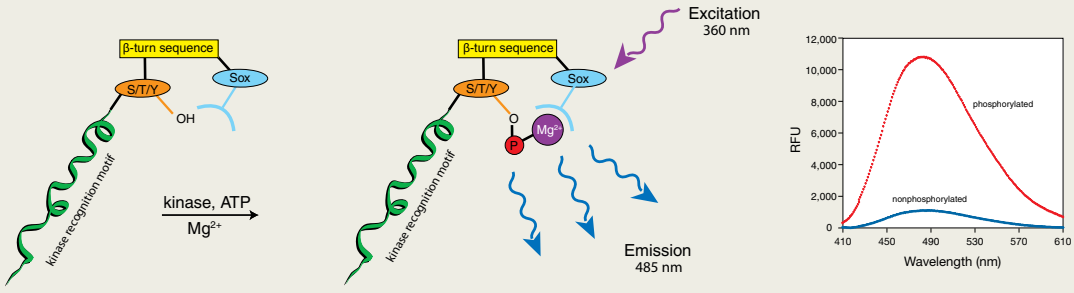

Figure 1—In the Omnia™ Kinase Assay platform, binding of Mg^{2+} and the Sox moiety results in increased fluorescence. These emission spectra illustrate the 2- to 10-fold increase in fluorescence signal between the nonphosphorylated peptide substrate (lower curve) and the fully phosphorylated peptide product (upper curve).

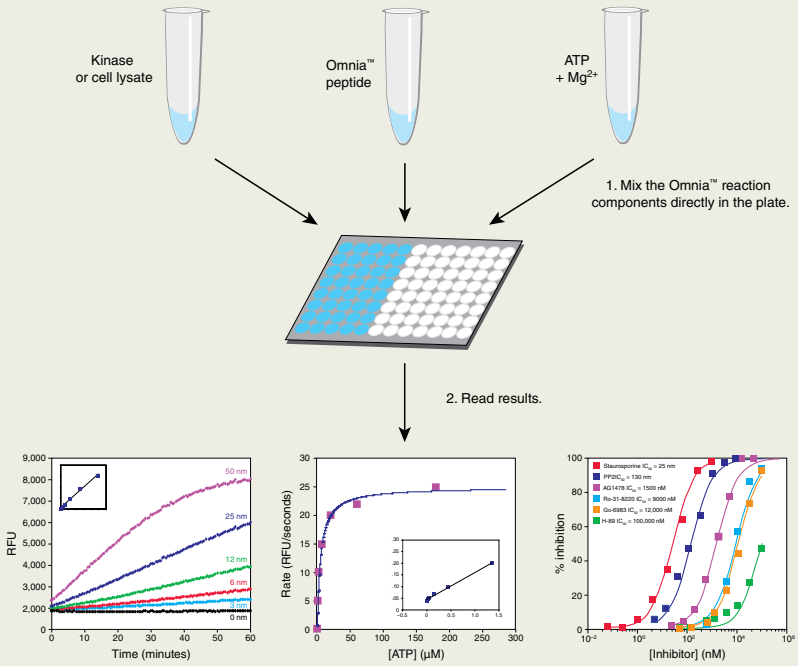

Figure 2—Simple two-step Omnia™ Kinase Assay procedure. Mix together the Omnia™ reaction components and record the fluoresence intensity in real time. Data can be analyzed for time-course studies, Hanes plots, IC_{50}, and more.

Ser, Thr, or Tyr residue within the peptide substrate. This stringent structure-function relationship eliminates interference from free phosphate or ATP in the reaction or from phosphorylation that may occur at other sites in the substrate (including the use of primed phosphopeptides as substrates), as often seen in other kinase assays.

In creating Omnia™ Kinase Assay substrates, the Sox fluorophore serves as an unnatural amino acid that can be made as an Fmoc derivative and thereby readily incorporated into the peptide substrate using standard solid-phase chemistry. The Sox fluorophore can be added at either the N- or C-terminus of the peptide substrate, where it is optimally positioned relative to the residue to be phosphorylated using an appropriate spacer-β turn sequence (i.e., Sox-Pro-Gly-X-Y-Z and Z-Y-X-dPro-Sox-Gly, respectively, where X is 0–2 amino acids derived from the substrate sequence, Y is the Ser, Thr, or Tyr residue, and Z is additional sequence required for efficient phosphorylation by the kinase of interest).

Assay procedure

The procedure for the Omnia™ Kinase Assays is extremely easy to perform, allowing detection of kinase activity in a homogeneous solution without using any exogenous components such as antibodies, beads, or stop solutions. Simply combine the reaction components directly in the assay plate and then read the fluorescence signal in a plate reader in kinetic mode (Figure 2).

Data are collected in real time for an appropriate time interval. Reaction conditions can be adjusted in many ways to directly alter the time required. Additionally, you can choose to collect data only at the beginning and the end of the assay to minimize reading time on the fluorescence plate reader. It is also possible to set up brief kinetic screens or to simply blank after adding compounds and all reaction components except the kinase. Once kinase is added, the plates can be subjected to a single time point reading, with or without the addition of a stop solution, to accommodate delays in reading the plates. In this manner, you can use one platform either in kinetic mode or as an endpoint assay.

Accurate activity measurement

Omnia™ Assays are ideal for performing different types of single and double titrations (e.g., enzyme, substrate, ATP, inhibitor, activator). With these determinations, accurate assessment of kinase thermodynamic or inhibitor parameters requires that the reaction be run at a constant steady-state rate. Because the enzyme activity in an Omnia™ Kinase Assay is

→

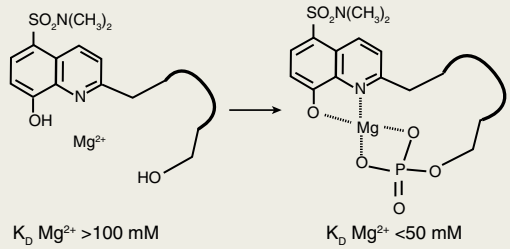

Figure 3—Minimal interference is intrinsic to the Sox moiety design. The chemical structure of the Omnia™ peptides prevents unwanted binding of reaction components.

continuously monitored in real time, data can be selected from the ideal region of the progress curve, resulting in more precise information. This approach greatly simplifies activity titration procedures, making it especially useful in K_i and drug mechanism/mode of action (MOA) determinations. The data precision from the Omnia™ Kinase Assay is superior to other types of assay platforms, even at very low percent conversion (Z′ values ≥0.8, Table 1). Moreover, the strong difference between the fluorescence signal from the phosphorylated and nonphosphorylated peptide provides excellent signal-to-noise ratios (generally 4- to 12-fold).

Minimal interference for precise results

The unique structural requirements (Figure 3) intrinsic to the peptide substrate and Sox moiety prevent interference from free phosphate, ATP, or other phosphorylated sites in the substrate or proteins found in the reaction mixture. This allows ATP concentrations up to 5 mM and for the use of primed phosphopeptides as substrates (as observed with kinases such as GSK3). By using the reaction rate information, the Omnia™ Kinase Assay can also eliminate interference caused by inhibitors that exhibit autofluorescence in the region used for excitation and emission, which often presents a major challenge in high-throughput screening of kinase inhibitors from small-molecule libraries (Figure 4).

Measure kinase activity in crude cell lysates

Because Omnia™ peptide substrates exhibit sufficiently high selectivity for the kinase of interest (this can be enhanced by the inclusion of off-target inhibitors), the Omnia™ platform can be used to measure kinase activity in crude cell lysates. As published by Shults et al.,[3] the Omnia™ Assay has been validated for detection of PKA, Akt, and MK2 in crude cell lysates made from cells treated with an appropriate stimulus or untreated. In each case, the signals obtained were dramatically reduced or eliminated with a selective kinase inhibitor. To corroborate this approach, we have developed a series of bead-based IP kinase assays, where a specific kinase or isoform is recovered from crude cell lysates on either a standard agarose or magnetic Dynabeads® particle immunoprecipitation step prior to running to the Omnia™ Kinase Assay.

Analyze cascade reactions

The Omnia™ Kinase Assay is also ideal for analyzing cascade reactions, as observed for MAPK (MAP3K→MAP2K→MAPK→MK) and Akt (PDK1→Akt).

Table 1—High-precision results achieved with the Omnia™ Kinase Assay.

% Conversion	Signal-to-background ratio	Signal-to-noise ratio	Z′ values	CV%
0	NA	NA	NA	4.20
2.5	1.15	2.10	0.67	5.10
5	1.31	4.00	0.77	5.00
10	1.61	6.84	0.82	4.90
15	1.91	7.81	0.78	5.70
20	2.22	12.11	0.88	4.10
50	4.08	18.54	0.88	3.90
100	6.97	18.91	0.86	4.50

Z′ values, CV%, and signal-to-background/noise ratios for the Omnia™ Assay for Akt at 10 µM substrate concentration. NA = not applicable.

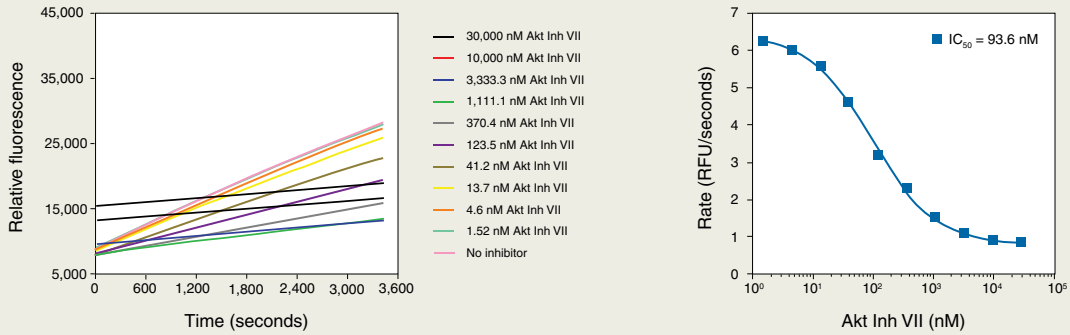

Figure 4—Ability of Omnia™ assays to correct for compound autofluorescence and provide the expected IC_{50} value. Interference from increasing concentrations of the autofluorescent AKT inhibitor VII (0–30,000 µM) is overcome by monitoring the reaction rate (change in fluorescence intensity over time) rather than an endpoint fluorescent signal. The IC_{50} for this inhibitor was determined to be 94 nM.

As shown in Figure 5, changes in p38 activity can readily be detected using increasing amounts of crude lysate (7.5–200 µg) made from treated cells. With this application, the kinetic readout of the Omnia™ format allows selection of the optimal window for looking at signaling via a variety of complexes formed in the presence (treated) or absence (basal) of stimulation.

Over 130 Omnia™ Kinase Assays available

The Omnia™ Kinase Assay is a simple-to-use assay platform that uses a series of Sox-based substrate peptides to measure the activity of a wide range of protein Ser/Thr and Tyr kinases. This assay can be adapted for most, if not all, kinase assays to accelerate progress and provide considerably more information. The kinetic format of the Omnia™ Assay readily corrects for any interference from other compounds that may be present in the reaction solution, producing results that correlate positively with those achieved using comparative fluorescence-based assays. Distinct

→

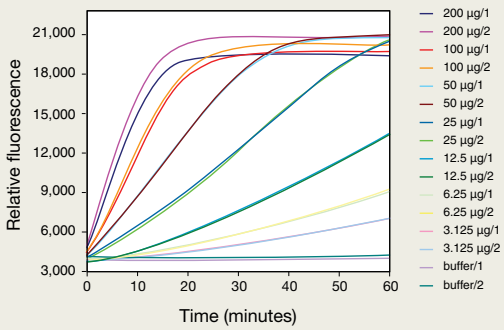

Figure 5—Omnia™ Assays enable cascade reaction studies within the optimal window for activity. The graph illustrates plate-captured p38 activity in cell lysate.

Find new tools for kinase discovery

Invitrogen offers a wide range of high-quality, innovative products and services to address key requirements of your drug discovery workflow. You'll find a full listing of kinase-related products, as well as current news, resources, and services, at our drug discovery web area. Visit **www.invitrogen.com/drugdiscovery** to learn more about our products for kinase discovery, including:

- Omnia™ Real-Time Kinase Assays
- LanthaScreen™ Time-Resolved FRET Assays
- Z-Lyte™ FRET Assays
- Recombinant kinases and phosphatases
- SelectScreen™ Kinase Profiling Service

advantages offered by the Omnia™ platform include measurement of kinase activity under optimal substrate concentrations and physiological (mM) ATP, and in real time without the use of radioactive tracers, beads, antibodies, development reagents, or specialized equipment. The Omnia™ platform has been used for the analysis of multiple sample types, including the determination of kinase activity of recombinant enzymes and the reconstruction of kinase cascades. These assays are also ideal for the analysis of substrate-competitive inhibitors, which is aided by the generally very low substrate K_m values. Omnia™ Assays are currently available for over 130 kinases, with more in progress. Table 2 lists the most popular assays. Learn more about how these important tools can help you rapidly increase your understanding of the kinome, and the manner in which the corresponding signaling pathways are regulated, at **www.invitrogen.com/omnia**. ■

References

1. Shults, M.D. et al. (2006) *Anal Biochem* 352:198–207.
2. Rothman, D.M. et al. (2005) *Trends Cell Biol* 15:502–510.
3. Shults, M.D. et al. (2005) *Nat Methods* 2:277–283.
4. Shults, M.D. and Imperiali, B. (2003) *J Am Chem Soc* 125:14248–14249.

Table 2—A selection of Omnia™ Kinase Assays.

Substrate	Validated kinase	Recombinant kits*	Bulk peptide substrate†
S/T 1	AKT1/2/3, CHK1, MLK2, MSK1, PAK1, PASK, PKA, PRKG2, RSK1/2/3, SGK1/2/3, ZIPK	KNZ2011	KNZ1011
S/T 2	AKT2, MLK2, MSK1, PAK1, PKA, PRKG1/2, PRKX, RSK2, SGK1/2/3	KNZ2021	KNZ1021
S/T 3	CHK1/2, MAPKAPK2/3/5, PHKG2, PKCμ, PKD2/3	KNZ2031	KNZ1031
S/T 4	AKT1/2/3, MLK2, MSK1, PAK1, PASK, PRKG2, RSK1, SGK1/2/3	KNZ2041	KNZ1041
S/T 5	AKT1/2/3, MLK2, MSK1, PAK1/4, PKA, PRKG1/2, PRKX, ROCK1/2, RSK1/2/3, SGK1/2/3	KNZ2051	KNZ1051
S/T 6	AKT1/2, MLK2, MSK1, p70S6K, PAK1, PASK, PKA, PRKX, RSK1/2/3, SGK1/2/3	KNZ2061	KNZ1061
S/T 7	CDK1/CyclinB, CDK2/CyclinA, CDK5/p35	KNZ2071	KNZ1071
S/T 8	MINK1, PKCα, PKCβI, PKCβII, PKCδ, PKCη, PKCι, PKCγ, PKCμ, PKCθ, PKCζ, PKD2/3	KNZ2081	KNZ1081
S/T 9	p38γ (MAPK12)	KNZ2091	KNZ1091
S/T 10	JNK1, p38δ , p38γ	KNZ2101	KNZ1101
S/T 11	CHK1/2, MAPKAPK3, PHKG2, PKCμ, PKD2, STK22D	KNZ2111	KNZ1111
S/T 12	TBK1	KNZ2121	KNZ1121
S/T 13	GSK3α, GSK3β	KNZ2131	KNZ1131
S/T 14	PIM2, ROCK1	KNZ2141	KNZ1141
S/T 15	CLK3, PASK, PHKG2, PIM2, PKCη	KNZ2151	KNZ1151
S/T 16	Aurora A	KNZ2161	KNZ1161
S/T 17	Erk1/2, p38γ	KNZ2171	KNZ1171
Y1	ABL1, CSF1R, EPHB2, FLT3, JAK2/3, LCK, LYNA, MERTK, MUSK, PDGFRα/ß	KNZ4011	KNZ3011
Y2	BLK, FER, FYN, LCK, LYNA, MERTK, TRKA, FAK, SRC	KNZ4021	KNZ3021
Y3	EPHA4, EPHB2, FAK, PTK1, SYK, VEGFR2	KNZ4031	KNZ3031
Y4	ABL1, ALK, FMS, FER, FLT3, IGF1R, IR, IRR, JAK2, MUSK, TRKA, PDGFR α/ß, ROS1	KNZ4041	KNZ3041
Y5	ABL1/2, BLK, BMX, BTK, EPHA2/8, EPHB2/3/4, FER, FGR, FLT3, FLT3 D835Y, FMS, FRK, FYN, HCK, IGF1R, LCK, LYNA, LYNB, MERTK, SYK, TRKB, YES	KNZ4051	KNZ3051
Y6	ABL1/2, ABL1 E225K, ABL1 G250E, ABL1 Y253F, BLK, EPHA1, EPHB1/2/3/4, FLT3, FMS, FRK, HCK, IGF1R, ITK LCK, MERTK, PDGFRβ, TRKB	KNZ4061	KNZ3061
Y7	ABL1, EGFR, EGFR L861Q, FGFR1, FGR, FLT3/4, FMS, FRK, JAK2/3, JAK2, JH1, JH2, V617F, RET, SYK, VEGFR1/2	KNZ4071	KNZ3071
Y8	FGFR1, FLT4, MST1R, PDGFRβ, RET, TEK, VEGFR1/2, YES, ZAP70	KNZ4081	KNZ3081

* Omnia™ Kinase Assay Recombinant Kits provide sufficient reagents for 100 × 50 µl or 250 × 20 µl reactions and include kinase reaction buffer, substrate peptide, ATP solution, DTT solution, phosphopeptide control, and a 96-well plate. † Omnia™ bulk substrates provide sufficient reagents for 400 × 50 µl or 1,000 × 20 µl reactions and include substrate peptide and phosphopeptide control.